

JAERI - M
89-046

NEANDC(J)-135/U
INDC(JPN)-122/L

EVALUATION OF NEUTRON NUCLEAR DATA OF B-11

April 1989

Tokio FUKAHORI

日本原子力研究所
Japan Atomic Energy Research Institute

JAERI-M レポートは、日本原子力研究所が不定期に公刊している研究報告書です。
入手の問合せは、日本原子力研究所技術情報部情報資料課（〒319-11茨城県那珂郡東海村）あて、お申しこしください。なお、このほかに財団法人原子力弘済会資料センター（〒319-11 茨城県那珂郡東海村日本原子力研究所内）で複数による実費領布をおこなっております。

JAERI-M reports are issued irregularly.

Inquiries about availability of the reports should be addressed to Information Division
Department of Technical Information, Japan Atomic Energy Research Institute, Tokai-mura,
Naka-gun, Ibaraki-ken 319-11, Japan.

©Japan Atomic Energy Research Institute, 1989

編集兼発行 日本原子力研究所
印 刷 いばらき印刷㈱

Evaluation of Neutron Nuclear Data of B-11

Tokio FUKAHORI

Department of Physics
Tokai Research Establishment
Japan Atomic Energy Research Institute
Tokai-mura, Naka-gun, Ibaraki-ken

(Received March 30, 1989)

Nuclear data of B-11 have been evaluated in the energy range from 0.01 meV to 20 MeV. The evaluated quantities are cross sections, angular distributions and energy spectra of secondary neutrons, and γ -ray data. The evaluation was performed by using the R-matrix theory below 7 MeV and multistep statistical model above 7 MeV. Below 7 MeV, R-matrix parameters of Koehler et al. were modified to fit experimental data of the total cross section. For calculation of the multistep statistical model, the optical model and the level density parameters were chosen to reproduce experimental data of charged particle emission and elastic scattering cross sections. Direct inelastic scattering processes for seven excited levels were considered with DWBA calculation. The results of present work are in good agreement with the experimental data of cross sections, angular distributions of secondary neutrons and double differential cross sections. They were compiled for JENDL-3 in the ENDF/B-V format.

Keywords: Evaluation, B-11, Neutron Nuclear Data, R-matrix,
Optical Model, DWBA, JENDL-3

¹¹Bの中性子核データの評価

日本原子力研究所東海研究所物理部

深堀 智生

(1989年3月30日受理)

入射中性子エネルギー 0.01 meV から 20 MeV の範囲で ¹¹B の中性子核データの評価を行った。評価した量は断面積、放出中性子の角度分布及びエネルギー・スペクトル、放出γ線のデータである。入射中性子エネルギー 7 MeV 以下では R 行列理論を用いて、7 MeV 以上では多段階統計模型を使用して評価を行った。7 MeV 以下については、Koehler らのパラメータを基に全断面積実験データを再現するように修正して R 行列パラメータを求めた。多段階統計模型の計算を行うに際して、光学模型パラメータ及び準位密度パラメータは弹性散乱及び荷電粒子放出反応断面積の実験データを再現するように決定した。DWBA 理論計算により 7 つの励起準位に関して直接過程の寄与を考慮した。評価結果は、断面積、放出中性子角度分布、二重微分断面積の実験データとよい一致を示した。評価結果は ENDF/B-V 形式で JENDL-3 に格納した。

Contents

1. Introduction	i
2. Evaluation below 7 MeV	1
2.1 R-matrix Calcualtion	1
2.2 Total Cross Section	2
2.3 Elastic Scattering Cross Section	2
2.4 Capture Cross Section	2
3. Evaluation above 7 MeV	3
3.1 Total and Elastic Scattering	3
3.2 Inelastic Scattering	3
3.3 Other Reactions	3
3.4 γ -ray Data	4
4. Results and Discussions	4
4.1 Cross Sections	4
4.2 Angular Distributions	5
4.3 Double Differential Cross Section	5
4.4 γ -ray Data	6
5. Conclusion	6
References	7

目 次

1. 緒 言	1
2. 入射中性子エネルギー 7 MeV以下の評価	1
2.1 R-行列法による計算	1
2.2 全断面積	2
2.3 弹性散乱断面積	2
2.4 捕獲反応断面積	2
3. 入射中性子エネルギー 7 MeV以上の評価	3
3.1 全断面積及び弹性散乱	3
3.2 非弹性散乱	3
3.3 その他の反応	3
3.4 γ 線データ	4
4. 評価結果及び議論	4
4.1 断面積	4
4.2 放出中性子角度分布	5
4.3 二重微分断面積	5
4.4 γ 線データ	6
5. 結 論	6
参考文献	7

1. Introduction

For the third version of the Japanese evaluated nuclear data library (JENDL-3), evaluation, compilation and revision have been continued. The evaluated nuclear data of B-11 are not included in JENDL-2, though they are necessary to calculate neutron transport in the light water reactor (LWR), neutron multiplication or tritium breeding of fusion reactors. A lot of experimental data of total cross section have been measured by many authors, but a few or no measurement for the other quantities of B-11 has been performed.

In this paper, the evaluation of neutron nuclear data of B-11 was performed in the neutron energy range from 0.01 meV to 20 MeV. The evaluated quantities, which are summarized in Table 1 with Q-values, were cross sections, angular distributions and energy spectra of secondary neutrons, and γ -ray data. Direct inelastic scattering processes were calculated for seven excited levels ($Q = -2.12, -4.45, -5.02, -6.74, -6.79, -9.12$ and -10.6 MeV) with the DWBA.

This paper consists of three parts. In Chapter 2, the energy range of incident neutron is below 7 MeV and evaluation of cross sections of total, elastic and inelastic scattering by using the R-matrix theory is described. Capture cross section was evaluated by using the multilevel Breit-Wigner (MLBW) formula. In Chapter 3, the energy range of incident neutron is above 7 MeV. Evaluation of the total, elastic and inelastic scattering, and other reaction cross sections, angular distributions and energy spectra of secondary neutrons, γ -ray production cross sections or multiplicities, and γ -ray spectra by using multistep statistical model and DWBA is explained. Results are shown and discussed in Chapter 4.

2. Evaluation below 7 MeV

2.1 R-matrix Calculation

Cross sections of total, elastic and inelastic scattering, and angular distributions of secondary neutrons were basically evaluated with the R-matrix theory. The calculations have been performed by using

the R-matrix calculation code RESCAL /1/. R-matrix parameters of Koehler et al./2/ were chosen as the initial values for calculation of elastic scattering and the first excited level ($Q = -2.12$ MeV) inelastic scattering cross sections. Initial values for parameters of the second and third excited levels ($Q = -4.45$ and -5.02 MeV) were assumed tentatively, and the all parameters were modified to fit experimental data of the total cross section measured by Mooring et al./3/, Porter et al./4/, Lane et al./5/, Cabe et al./6/, and Auchampaugh et al./22/. The results of R-matrix parameters are shown in Table 2 with the parameters of Koehler et al.

2.2 Total Cross Section

Below 0.1 MeV, the total cross section was calculated with the multilevel Breit-Wigner (MLBW) formula and the resonance parameters taken from the values of Mughabghab et al./8/. The cross section was evaluated by using the R-matrix calculation in the energy range of 0.1 to 4 MeV. Above 4 MeV, smooth curve of the total cross section was obtained by fitting it to the experimental data of Auchampaugh et al.

2.3 Elastic Scattering Cross Section

Below 0.1 MeV, the elastic scattering cross section was based on the MLBW formula and the resonance parameters taken from the values of Mughabghab et al. The cross section was evaluated by using the R-matrix calculation in the energy range of 0.1 to 2.2 MeV. Above 2.2 MeV, the cross section was obtained by subtracting the inelastic scattering and the capture cross sections from the total cross section.

2.4 Capture Cross Section

The capture cross section was calculated basically with the MLBW formula by adopting resonance parameters recommended by Mughabghab et al. The direct capture cross section /8/ was added to them. That was also adopted in the energy range up to 20 MeV.

3. Evaluation above 7 MeV

3.1 Total and Elastic Scattering

The total cross section was obtained by tracing to the experimental data of Auchampaugh et al. above 4 MeV.

The elastic scattering cross section above 2.2 MeV was obtained by subtracting the reaction cross sections from the total cross section.

For the elastic scattering, the angular distribution of the secondary neutrons was calculated by using the statistical model code CASTHY /9/ and the DWBA code DWUCK4/10/ above 7 MeV. The results of two codes were added with the weight of cross sections.

3.2 Inelastic Scattering

Direct inelastic scattering processes for seven excited levels ($Q = -2.12, -4.45, -5.02, -6.74, -6.79, -9.12$ and -10.60 MeV) were considered. The calculation was performed with DWUCK4. The multistep statistical model code GNASH/11/ was also used to calculate the cross sections and the angular distributions of the inelastic scattering.

The direct inelastic scattering cross section was added to compound one to reproduce the experimental data of cross sections and angular distributions measured by Koehler et al., Glendinning et al./12/, and those of the double differential cross section of Takahashi et al./7/.

Excited levels were assumed to be overlapping above 7.2 MeV. Calculation of cross section of continuum inelastic scattering was performed by the GNASH code.

3.3 Other Reactions

The reaction cross sections ($(n,2n)$, (n,p) , (n,d) , (n,α) , (n,np) , (n,nd) , (n,nt) and $(n,n\alpha)$) and the energy spectra of secondary neutrons were calculated with the GNASH code. For the GNASH calculation, the optical model and the level density parameters were adjusted so that the calculation could reproduce the experimental data of the (n,p) , (n,d) , (n,t) , and (n,α) reaction and elastic scattering cross sections. The parameters are shown in Tables 3 and 4. The level scheme using in the GNASH calculation are shown in Table 5. Calculated cross sections of the

(n,p) and (n, α) reactions were normalized to the experimental data of Stepancic et al./13/, and those of Antolkovic et al./14/ and Scobel et al./15/, respectively.

Cross section and energy spectrum of the (n,n 2α) reaction were evaluated by adopting those shapes of the (n,nt) reaction and normalizing them to the experimental data of the helium production cross section of Kneff et al./16/.

3.4 γ -ray Data

The multiplicities of capture and inelastic scattering to the seven discrete levels were calculated by using the GNASH code below 7.8 MeV. Above 7.8 MeV, the γ -ray production cross sections of non-elastic scattering including all reaction and inelastic scattering were calculated by using GNASH code. The γ -ray spectra were also obtained by GNASH calculation.

4. Results and Discussions

4.1 Cross Sections

The total cross section calculated with R-matrix in the energy range from 0.2 to 6.0 MeV is shown in Fig.1. The solid and dashed lines mean the present work and ENDF/B-IV, respectively. The present result is in good agreement with the experimental data.

Figures 2-4 show the (n,p), (n, α), and (n,2n) cross sections as examples of the reaction cross sections calculated by using the GNASH code. The lines are the same as Fig.1. The results of the (n,p) and (n, α) reactions reproduce the experimental data. The (n,2n) reaction does not agree with Mather et al.'s data which the present evaluation did not adopt the data.

As an example of calculation with the statistical model and the DWBA, the inelastic scattering cross sections of the first four excited levels are illustrated in Fig.5. The solid, dashed, and dash-dotted lines mean the present work, ENDF/B-IV, and the calculation with the R-matrix parameters of Koehler et al., respectively. The ratio of the

compound process to the direct process was assumed to be 0.8 in the whole energy range. The present results reproduce the experimental data.

The total helium production cross section is composed of the (n,α) , $(n,n\alpha)$, $(n,n2\alpha)$, and (n,nt) cross sections and illustrated in Fig.6 compared with the experimental data of Kneff et al./16/. The solid line means the present work and the dashed line means the helium production cross section of ENDF/B-IV. The present result is in good agreement with the experimental data.

4.2 Angular Distributions

The angular distributions of elastically scattered neutrons at the incident neutron energies of 4.00, 7.98 and 13.94 MeV are shown in Fig.7. The solid, dashed, and dash-dotted lines describe the present work, and ENDF/B-IV, respectively. The present result at $E_n = 4.00$ MeV was calculated with R-matrix and the calculations at 7.98 and 13.94 MeV were performed with DWUCK4 and GNASH. The results reproduce the experimental data.

Figure 8 shows the inelastic angular distributions of the first three excited levels. The lines mean the same as Fig.7. Calculation was carried out with R-matrix below the incident neutron energy of 7 MeV and with DWUCK4 and GNASH above that of 7 MeV. The present work agrees with the experimental data.

The angular distributions of the secondary neutrons for the other reactions were assumed to be isotropic in the center of mass system.

4.3 Double Differential Cross Section

The double differential cross sections (DDX) are shown in Fig.9-10 compared with the experimental data measured at Osaka University (OKTAVIAN)/7/, and Tohoku University/25/. The DDX are compared with the experimental data of Los Alamos/27,28/ also. The peaks of elastic and inelastic scattering are in good agreement with the experimental data. In the lower energy region of secondary neutrons, the present result is much smaller than the experimental data, because the (n,nd) , (n,nt) and $(n,n2\alpha)$ reactions are not included in the calculation.

4.4 γ -ray Data

Figure 11 shows the γ -ray production cross section for the γ -ray energy of 2.125 MeV, comparing with the experimental data of Dickens et al./37/. The present result calculated from the γ -ray multiplicities of the inelastic scattering is a little larger than the experimental data. But the evaluated inelastic scattering cross sections reproduce the experimental data of the cross section.

5. Conclusion

The evaluation of neutron nuclear data of B-11 has been performed in the energy range from 0.01 MeV to 20 MeV. The evaluation was basically carried out by using the R-matrix, the statistical model, and the DWBA calculation. The results are in good agreement with the experimental data. The present work was compiled for JENDL-3 in the ENDF/B-V format.

REFERENCES

- 1) Komoda, S. et al.; private communication.
- 2) Koehler, P.E., Knox, H.D., Resler, D.A., Lane, R.O. and Millener, P.E.; Nucl. Phys. A394 (1983) 221
- 3) Mooring, F.P. et al.; Nucl. Phys. 82 (1966) 16
- 4) Porter, D. et al.; AWRE-O-45/70 (1970)
- 5) Lane, R.D. et al.; Phys. Rev. C2 (1970) 2097
- 6) Cabe, J. et al.; CEA-R-4524 (1973)
- 7) Takahashi, A. et al.; INDC(JPN)-106/L (1986)
- 8) Mughabghab, S.F., Divadeenam, M. and Holden, N.E.; 'Neutron Cross Sections' Vol.1 Part A (Academic Press 1981, New York)
- 9) Igarasi, S.; J. Nucl. Sci. Technol. 12 (1975) 67
- 10) Kunz, P.D.; unpublished
- 11) Young, P.G. and Arthur, E.D.; GNASH, A pre-equilibrium, Statistical Nuclear-Model Code for Calculation of Cross Section and Emission Spectra, LA-6947 (1977).
- 12) Glendinning, S.G. et al.; Bull. Am. Phys. Soc. 24 (1979) 656
- 13) Stepancic, B.Z. et al.; Bull. Inst. Boris Kidric 17 (1966) 237
- 14) Antolkovic, B. et al.; Nucl. Phys. A325 (1979) 189
- 15) Scobel, W. et al.; Zeitschrift f. Natur-forschung, A25 (1970) 1406
- 16) Kneff, D.W., Oliver, B.M. and Harry Farrar IV; Nucl. Sci. Eng. 92 (1986) 491
- 17) Glendinning, S.G., El-Kadi, S., Nelson, C.E., Pedroni, R.S., Purser, F.O. and Walter, R.L.; ibid. 80 (1982) 256
- 18) Watson, B.A., Singh, P.P. and Segel, R.E.; Phys. Rev. 182 (1969) 977
- 19) Miljanic, D. and Valkovic, V.; Nucl. Phys. A176 (1971) 110
- 20) Herling, G.H., Cohen, L. and Silverstein, J.D.; Phys. Rev. 178 (1969) 178
- 21) Matsuki, S., Yamashita, S., Fukunaga, K., Nguyen, D.C., Fujiwara, N. and Yanabu, T.; J. Phys. Soc. Japan 26 (1969) 1344
- 22) Auchampaugh, G.F., Plattard, S. and Hill, N.W.; Nucl. Sci. Eng. 69 (1979) 30
- 23) Kantele, J. et al.; Nucl. Phys. 35 (1962) 353

- 24) Strain, J.E. et al.; ORNL-3672 (1965)
- 25) Baba, M. et al.; NETU-47, Tohoku Univ. (1986)
- 26) Flesch, F. et al.; Oesterr. Akad. Wiss., Math.-Naturw. Kl.,
Sitzungsber. 176 (1966) 45
- 27) Drosig, M. et al.; LA-10665-MS (1986)
- 28) Drosig, M. et al.; Rad. Eff. 92 (1986) 145
- 29) Roturier, J. et al.; not published (1968)
- 30) Alder, J.C. et al.; Nucl. Phys. A147 (1969) 657
- 31) Hopkins, J.C. et al.; Nucl. Sci. Eng. 36 (1969) 275
- 32) Besotosnyj, et al.; Jadernye Konstanty, Obninsk Report 19 (1975)
77
- 33) White, R.M. et al.; Nucl. Phys. A340 (1980) 13
- 34) Hyakutake, M. et al.; NEANDC(J)-13 (1969) 29
- 35) Ajzenberg-Selove, F.; Nucl. Phys. A413 (1984) 1
- 36) Ajzenberg-Selove, F.; Nucl. Phys. A433 (1985) 1
- 37) Dickens, J.K. and Larson, D.C.; Proc. of International Conference
on Nuclear Science and Technology (1988 MITO) 213
- 38) Mather, D.S. et al.; AWRE-O-47/69 (1969)
- 39) Baba, M. et al.; Proc. of International Conference at Santa Fe
(1985)

Table 1 The Evaluated Quantities. Symbol "0" means that the evaluation was performed.

Quantities	σ	$d\sigma/d\Omega$	$d\sigma/dE$	γ -ray data	Q-values [MeV]
total	0	-	-	-	-
elastic	0	0	-	-	0.0
non-elastic	-	-	-	0	-7.20
capture	0	-	-	0	3.396
inelastic	0	0	0	0	-2.12
(n,2n)	0	0	0	-	-11.46
(n,p)	0	-	-	-	-10.73
(n,d)	0	-	-	-	-9.00
(n,t)	0	-	-	-	-9.56
(n, α)	0	-	-	-	-6.63
(n,np)	0	0	0	-	-11.23
(n,nd)	0	0	0	-	-15.82
(n,nt)	0	0	0	-	-11.22
(n,n α)	0	0	0	-	-8.67
(n,n2 α)	0	0	0	-	-11.13

Table 2 (a) R-matrix Parameters for Elastic Scattering

(Q = 0.0 MeV, I π = 3/2-)

J π	λ	E λ	Koehler et al./2/			λ	E λ	Present Work		
0+			1	1				1	1	
			j	3/2				j	3/2	
			R ∞	0.2				R ∞	0.200	
0-			1	2				1	2	
			j	3/2				j	3/2	
			R ∞	0.3				R ∞	0.300	
1+			1	1	1			1	1	1
			j	1/2	3/2			j	1/2	3/2
			R ∞	0.2	0.2			R ∞	0.275	0.0
1	1.60	γ_1	0.1	0.25		1	1.600	γ_1	0.175	0.194
2	3.20	γ_2	-0.2	0.2		2	3.199	γ_2	-0.306	0.017
1-			1	0	2	2		1	0	2
			j	1/2	3/2	5/2		j	1/2	3/2
			R ∞	-0.1	0.3	0.25		R ∞	-0.185	0.290
1	-1.34	γ_1	0.85	0.0	0.0	1	-1.340	γ_1	0.850	0.030
2	0.935	γ_2	0.07	0.0	0.0	2	0.935	γ_2	0.070	0.004
3	2.45	γ_3	0.15	0.90	0.20	3	2.451	γ_3	0.147	0.900
4	3.70	γ_4	0.25	0.12	-0.36	4	3.705	γ_4	0.251	0.006
5	4.50	γ_5	0.20	-0.40	0.30	5	4.500	γ_5	0.200	-0.400
6	4.60	γ_6	0.25	0.55	0.25	6	4.601	γ_6	0.251	0.549
7	5.78	γ_7	0.0	0.0	-0.45	7	5.780	γ_7	0.0	0.158
2+			1	1	1			1	1	1
			j	1/2	3/2			j	1/2	3/2
			R ∞	0.2	0.2			R ∞	0.231	0.297
1	0.31	γ_1	0.12	0.40		1	0.345	γ_1	0.001	0.350

Table 2 (a) (continued)

$J\pi$	λ	$E\lambda$	Koehler et al./2/				λ	$E\lambda$	Present Work			
2-			1	0	2	2			1	0	2	2
			j	1/2	3/2	5/2			j	1/2	3/2	5/2
			R _∞	-0.1	0.3	0.25			R _∞	-0.100	0.304	0.250
1	-2.48	γ_1	0.8	0.0	0.0		1	-2.480	γ_1	0.800	0.004	0.003
2	0.638	γ_2	0.4	0.0	0.85		2	0.638	γ_2	0.400	0.003	0.850
3	4.40	γ_3	0.20	0.30	0.30		3	4.400	γ_3	0.200	0.300	0.300
4	5.76	γ_4	0.0	0.17	-0.17		4	5.760	γ_4	0.0	0.170	0.170
3+			1	1					1	1		
			j	3/2					j	3/2		
			R _∞	0.2					R _∞	0.326		
1	2.19	γ_1	0.265				1	2.190	γ_1	0.328		
3-			1	2	2				1	2	2	
			j	3/2	5/2				j	3/2	5/2	
			R _∞	0.3	0.25				R _∞	0.507	0.375	
1	-0.34	γ_1	0.0	0.60			1	-0.340	γ_1	0.100	0.635	
2	2.175	γ_2	0.19	0.19			2	2.150	γ_2	0.173	0.216	
3	4.87	γ_3	-0.35	0.10			3	4.871	γ_3	-0.432	0.0	
4	4.94	γ_4	0.15	0.15			4	4.915	γ_4	0.668	0.0	
5	5.24	γ_5	0.2	0.2			5	5.150	γ_5	0.179	0.326	
6	5.40	γ_6	-0.20	-0.20			6	5.352	γ_6	-0.001	-0.335	
7	6.50	γ_7	0.20	0.0			7	6.502	γ_7	0.306	0.003	
4-			1	2					1	2		
			j	5/2					j	5/2		
			R _∞	0.25					R _∞	0.804		
1	0.644	γ_1	1.00				1	0.325	γ_1	1.309		
							2	7.160	γ_2	0.519		

Table 2 (b) R-matrix Parameters for Inelastic Scattering of the First
Excited Level $(Q = -2.12 \text{ MeV}, I\pi = 1/2^-)$

$J\pi$	λ	$E\lambda$	Koehler et al./2/			λ	$E\lambda$	Present Work		
0+			1	1				1	1	
			j	1/2				j	1/2	
			R ∞	0.1				R ∞	0.100	
0-			1	0				1	0	
			j	1/2				j	1/2	
			R ∞	0.1				R ∞	0.100	
1+			1	1	1			1	1	1
			j	1/2	3/2			j	1/2	3/2
			R ∞	0.1	0.1			R ∞	0.082	0.155
	1	1.60	γ_1	0.0	0.0	1	1.600	γ_1	0.0	0.0
	2	3.20	γ_2	0.20	0.0	2	3.199	γ_2	0.201	0.097
1-			1	0	2			1	0	2
			j	1/2	3/2			j	1/2	3/2
			R ∞	0.1	0.1			R ∞	4.690	1.060
	1	-1.34	γ_1	0.0	0.0	1	-1.340	γ_1	0.0	0.0
	2	0.935	γ_2	0.0	0.0	2	0.935	γ_2	0.0	0.0
	3	2.45	γ_3	0.10	0.50	3	2.451	γ_3	0.096	0.498
	4	3.70	γ_4	0.0	0.10	4	3.705	γ_4	0.099	0.107
	5	4.50	γ_5	0.0	0.40	5	4.500	γ_5	0.011	0.400
	6	4.60	γ_6	-0.30	0.0	6	4.601	γ_6	-0.299	0.009
	7	5.78	γ_7	-0.50	-0.20	7	5.780	γ_7	-0.005	-0.008
2+			1	1				1	1	
			j	3/2				j	3/2	
			R ∞	0.1				R ∞	0.100	
1	0.31	γ_1	0.0			1	0.345	γ_1	0.0	

Table 2 (b) (continued)

$J\pi$	λ	$E\lambda$	Koehler et al./2/			λ	$E\lambda$	Present Work		
2-			1	2	2			1	2	2
			j	3/2	5/2			j	3/2	5/2
			R ∞	0.1	0.1			R ∞	0.506	0.015
1	-2.48	γ_1	0.0	0.0		1	-2.480	γ_1	0.0	0.0
2	0.638	γ_2	0.0	0.0		2	0.638	γ_2	0.0	0.0
3	4.40	γ_3	-0.24	-0.50		3	4.400	γ_3	-0.240	-0.499
4	5.76	γ_4	0.0	0.15		4	5.760	γ_4	0.018	0.014
3-			1	2				1	2	
			j	5/2				j	5/2	
			R ∞	0.1				R ∞	1.843	
1	-0.34	γ_1	0.0			1	-0.340	γ_1	0.0	
2	2.175	γ_2	0.65			2	2.150	γ_2	0.0	
3	4.87	γ_3	0.50			3	4.871	γ_3	0.237	
4	4.94	γ_4	0.0			4	4.915	γ_4	0.396	
5	5.24	γ_5	0.2			5	5.150	γ_5	0.048	
6	5.40	γ_6	0.30			6	5.352	γ_6	0.474	
7	6.50	γ_7	0.60			7	6.502	γ_7	0.167	

Table 2 (c) R-matrix Parameters for Inelastic Scattering of the Second and Third Excited Levels

$J\pi$	λ	$E\lambda$	$Q=-4.45 \text{ MeV}, 5/2^-$			$Q=-5.02 \text{ MeV}, 3/2^-$		
1+			1	1		1	1	
			j	3/2		1/2	3/2	
			R ∞	0.100		0.100	0.100	
1-			1	2	2	0	2	2
			j	3/2	5/2	1/2	3/2	5/2
			R ∞	0.001	0.299	-0.177	0.187	0.188
1	-1.340	γ_1	0.0	0.0		0.0	0.0	0.0
2	0.935	γ_2	0.0	0.0		0.0	0.0	0.0
3	2.451	γ_3	0.0	0.0		0.0	0.0	0.0
4	3.705	γ_4	0.0	0.0		0.0	0.0	0.0
5	4.500	γ_5	0.094	0.080		0.0	0.0	0.0
6	4.601	γ_6	0.093	0.099		0.0	0.0	0.0
7	5.780	γ_7	0.288	0.030		0.003	0.122	0.001
2+			1	1	1	1	1	
			j	1/2	3/2	1/2	3/2	
			R ∞	0.100	0.100	0.100	0.100	
2-			1	0	2	2	0	2
			j	1/2	3/2	5/2	1/2	3/2
			R ∞	0.093	0.047	0.078	0.136	0.080
1	-2.480	γ_1	0.0	0.0	0.0	0.0	0.0	0.0
2	0.638	γ_2	0.0	0.0	0.0	0.0	0.0	0.0
3	4.400	γ_3	0.070	0.085	0.107	0.0	0.0	0.0
4	5.760	γ_4	0.004	0.0	0.009	0.002	0.0	0.346

Table 2 (c) (continued)

$J\pi$	λ	$E\lambda$	$Q=-4.45 \text{ MeV}, 5/2^-$			$Q=-5.02 \text{ MeV}, 3/2^-$	
3+		1	1	1		1	
		j	1/2	3/2		3/2	
		R_∞	0.100	0.100		0.100	
3-		1	0	2	2	2	2
		j	1/2	3/2	5/2	3/2	5/2
		R_∞	0.093	0.047	0.078	0.080	0.080
1	-0.340	γ_1	0.0	0.0	0.0	0.0	0.0
2	2.150	γ_2	0.0	0.0	0.0	0.0	0.0
3	4.871	γ_3	0.053	0.017	0.169	0.0	0.0
4	4.915	γ_4	0.039	0.167	0.022	0.0	0.0
5	5.150	γ_5	0.141	0.181	0.003	0.189	0.121
6	5.352	γ_6	0.048	0.045	0.067	0.006	0.092
7	6.502	γ_7	0.015	0.0	0.404	0.376	0.0
4-		1	2	2		2	
		j	3/2	5/2		5/2	
		R_∞	0.050	0.050		0.025	
1	0.325	γ_1	0.0	0.0		0.0	
2	7.160	γ_2	0.020	0.045		0.047	

Table 3 The Optical Potential Parameters

neutron	V =41.8-0.005E*	r0=1.40	a0=0.35	/17/
	Ws=1.01E	*	rI=1.15*	aI=0.50
proton	V =66.1-0.273E	r0=1.15	a0=0.57	/18/
	Ws=1.50+0.581E	rI=1.15	aI=0.5	
	Vsym=5.5	r0=1.15	a0=0.57	
deuteron	V =80.0	*	r0=1.0 *	a0=1.0 *
	Wv=30.0		rI=1.0 *	aI=0.8 *
	Vsym =6.0	*	r0=1.0 *	a0=1.0 *
triton	V =103.0+20.0E*	r0=0.85	a0=0.70	/20/
	Wv=1.49E	*	rI=2.06	aI=0.72
	Vsym =8.55	*	r0=0.85	a0=0.70
alpha	V =285.2-2.40E*	r0=1.61*	a0=0.55*	/21/
	Ws=16.16-0.70E*	rI=1.81	aI=0.65	

NOTE : E is incident neutron energy in LAB. system
 with units of MeV and fm. * means that parameter
 is modified from original one.

Table 4 The Level Density Parameters

	a[1/MeV]	T[MeV]	Pair.[MeV]
B-10	1.196	7.990	0.0
B-11	1.431	6.112	2.67
B-12	1.491	6.201	0.0
Be-8	1.115	9.187	2.13
Be-9	1.125	8.248	2.46
Be-10	1.088	10.029	5.13
Be-11	1.419	7.277	2.46
Li-7	1.138	7.197	2.67
Li-8	1.115	8.170	0.0

Table 5 The Adopted Level Scheme /35, 36/

	^{10}B		^{11}B		^{12}B		^8Be		^9Be	
gs	0.0	3+	0.0	3/2-	0.0	1+	0.0	0+	0.0	3/2-
1	0.718	1+	2.125	1/2-	0.953	2+	3.040	2+		
2	1.740	0+	4.445	5/2-	1.674	2-				
3	2.154	1+	5.020	3/2-	2.621	1-				
4	3.587	2+	6.743	7/2-	2.720	0+				
5	4.774	3+	6.792	1/2+						
6	5.110	2-	9.120	7/2+						
7	5.164	2+	10.60	7/2+						
8	5.180	1+								
9	5.926	2+								
10	6.025	4+								
11	6.127	3-								
12	6.561	4-								

	^{10}Be		^{11}Be		^7Li		^8Li	
gs	0.0	0+	0.0	1/2+	0.0	3/2-	0.0	2+
1	3.368	2+	0.320	1/2-	0.478	1/2-	0.981	1+
2	5.958	2+			4.630	7/2-		
3	5.960	1-			6.680	5/2-		
4	6.179	0+			7.456	5/2-		
5	6.263	2-						

NOTE: The energy is unit in MeV.

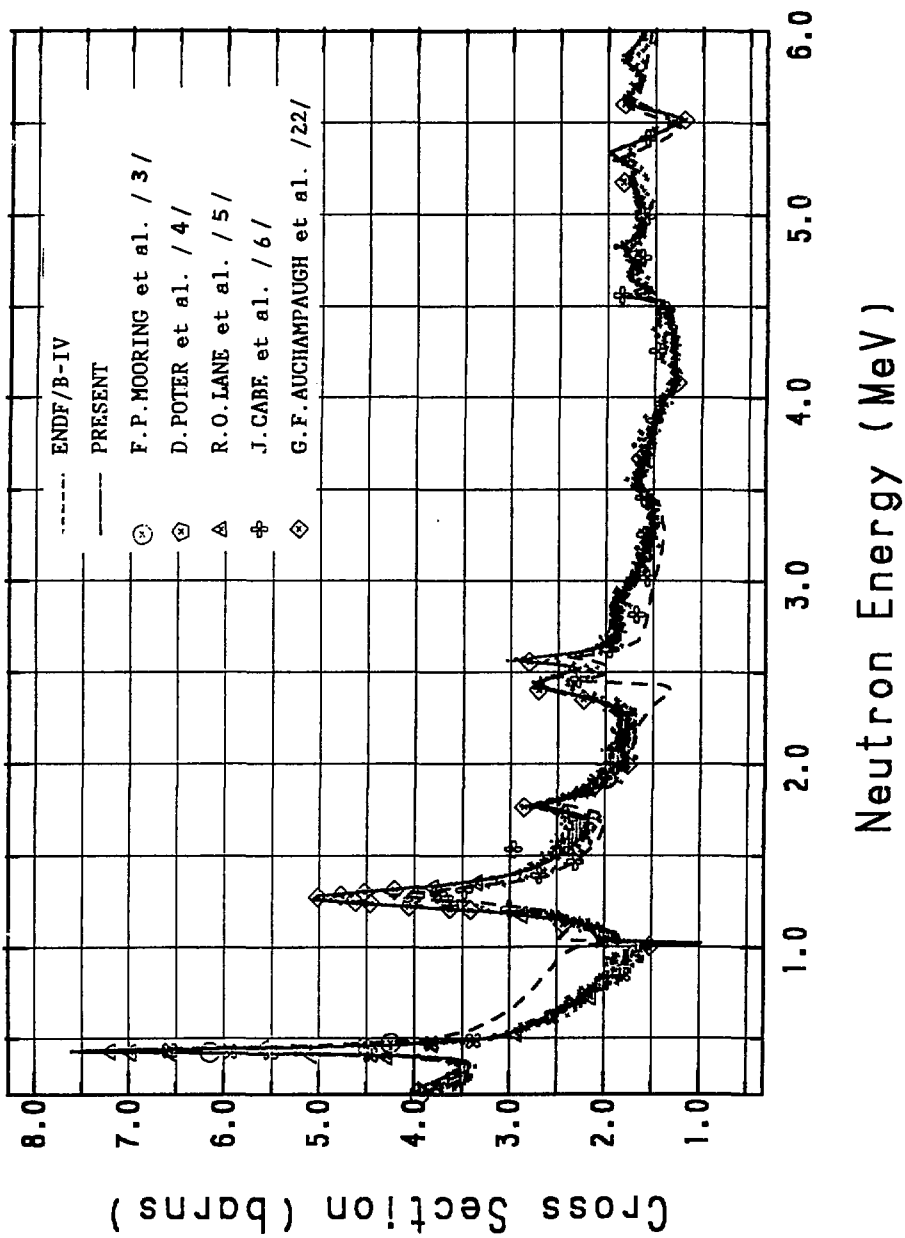


Fig.1 Total Cross Section

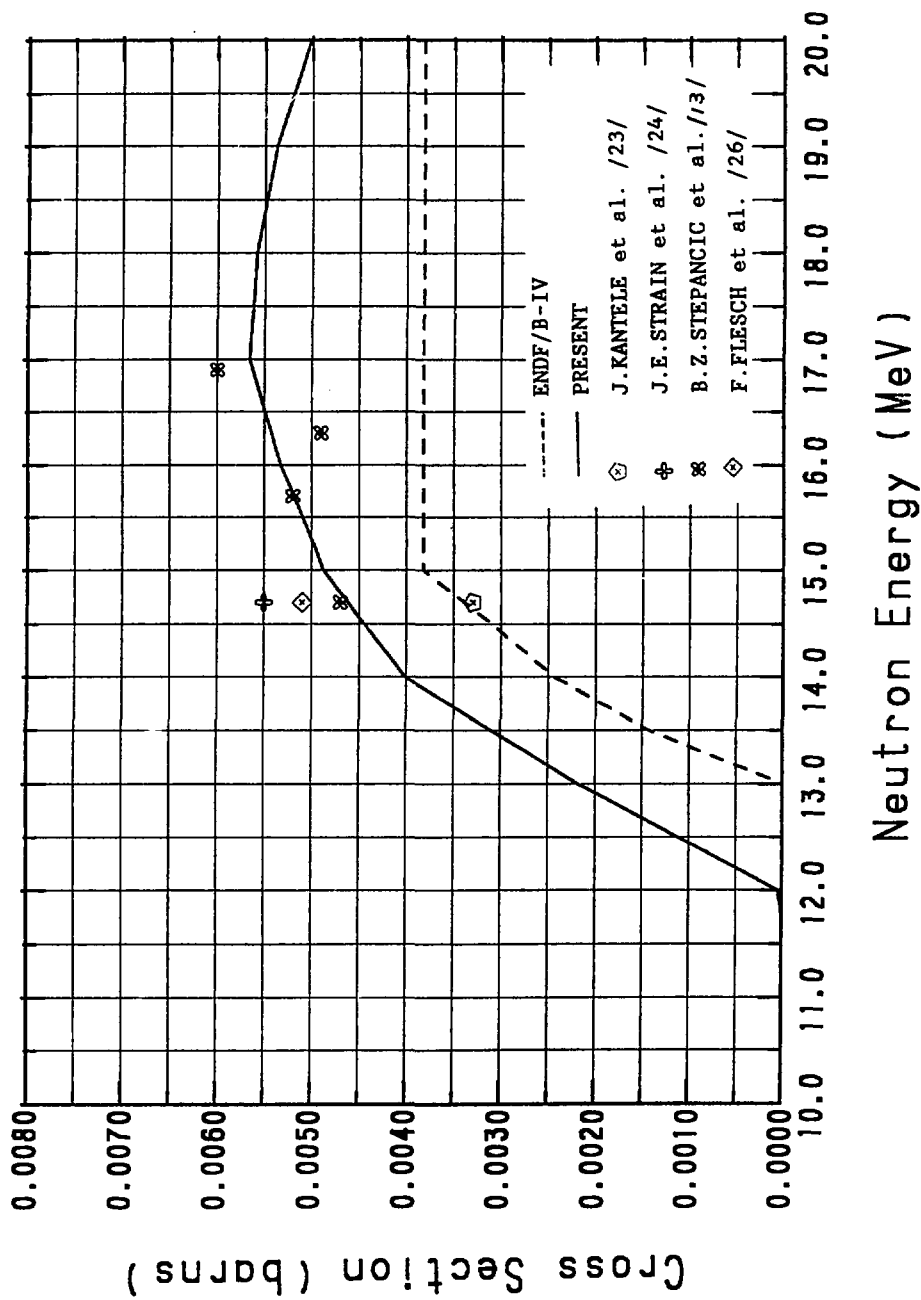


Fig. 2 (n,p) Cross Section

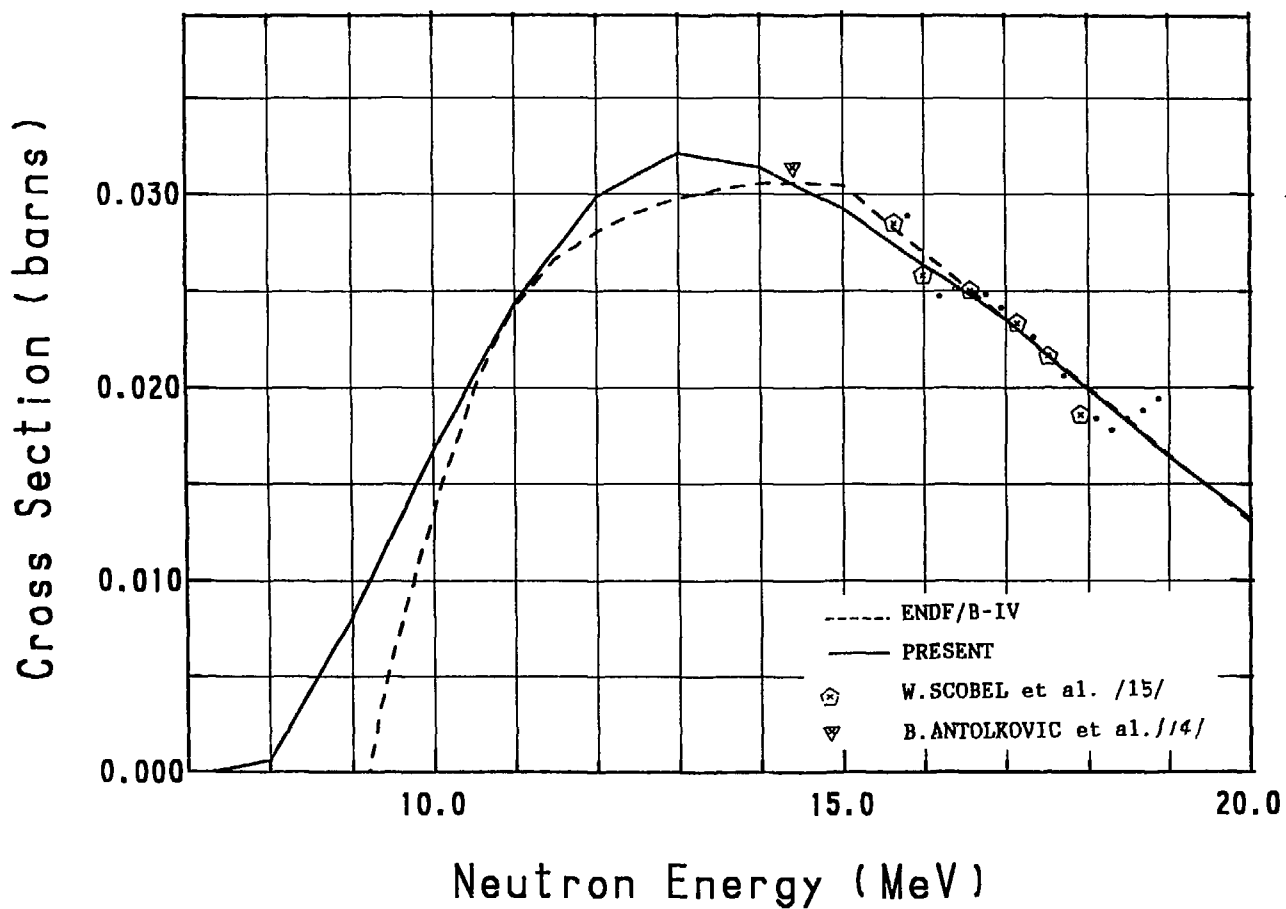


Fig. 3 (n,α) Cross Section

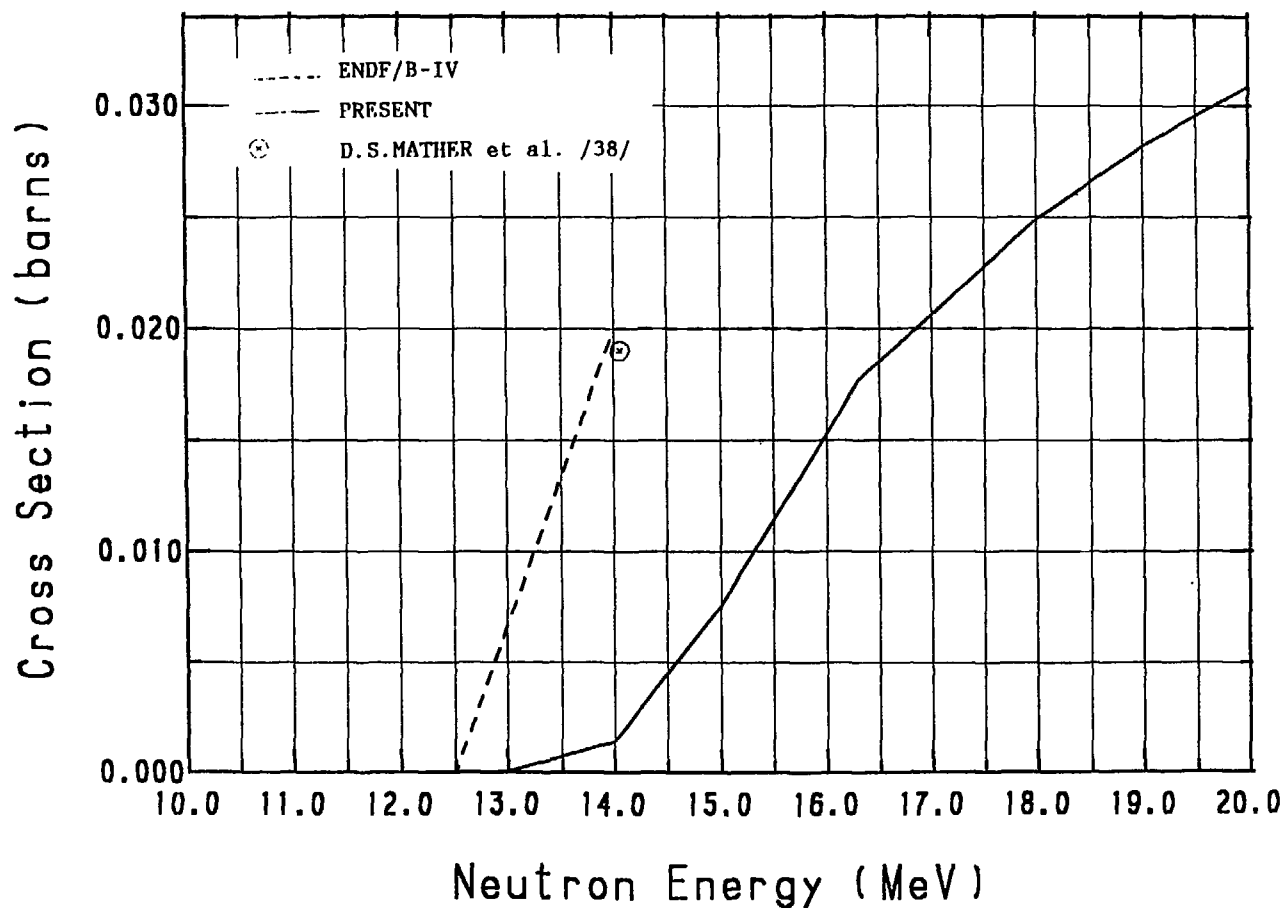


Fig.4 (n,2n) Cross Section

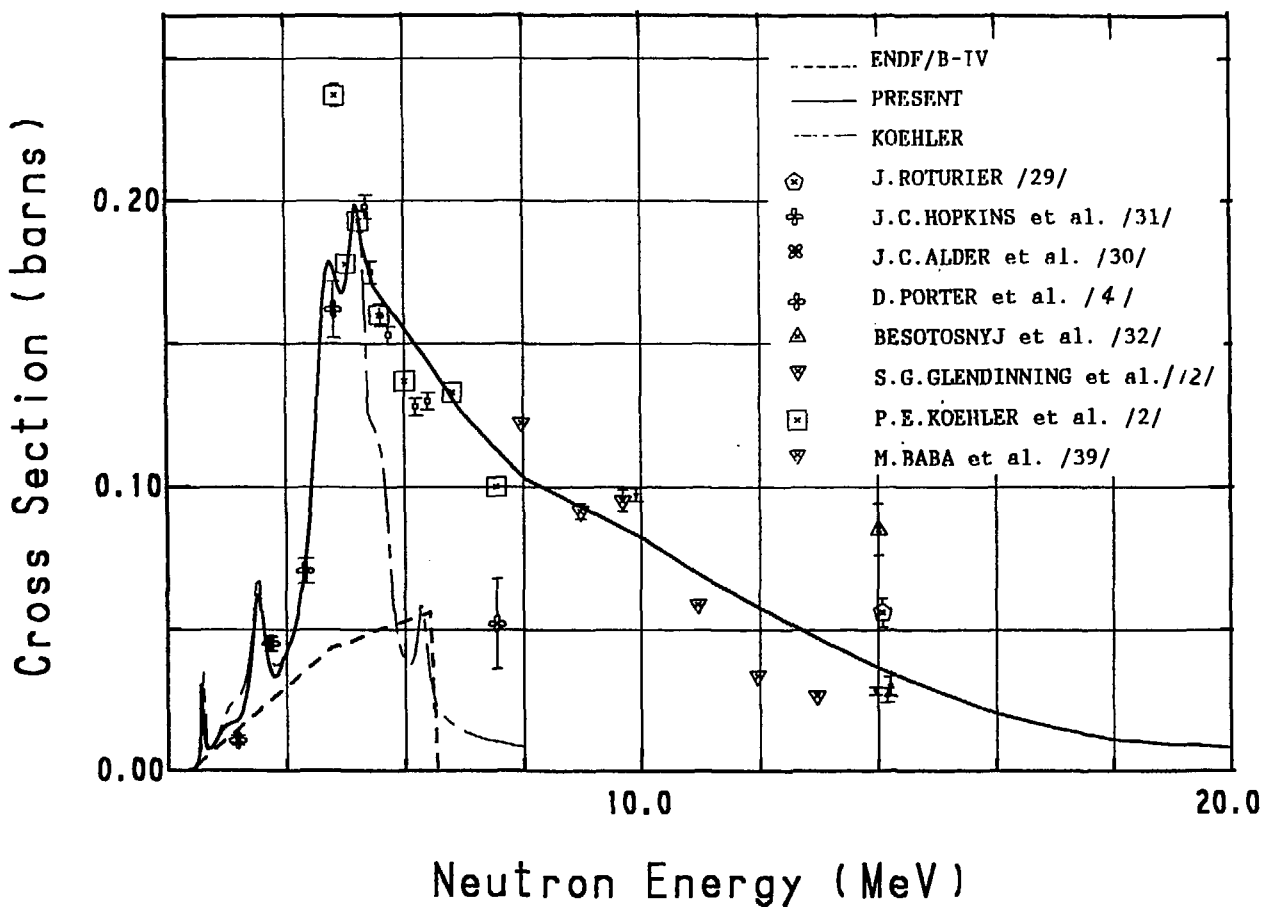


Fig.5 (a) Inelastic Scattering Cross Sections of the First Excited Level ($Q=-2.12$ MeV)

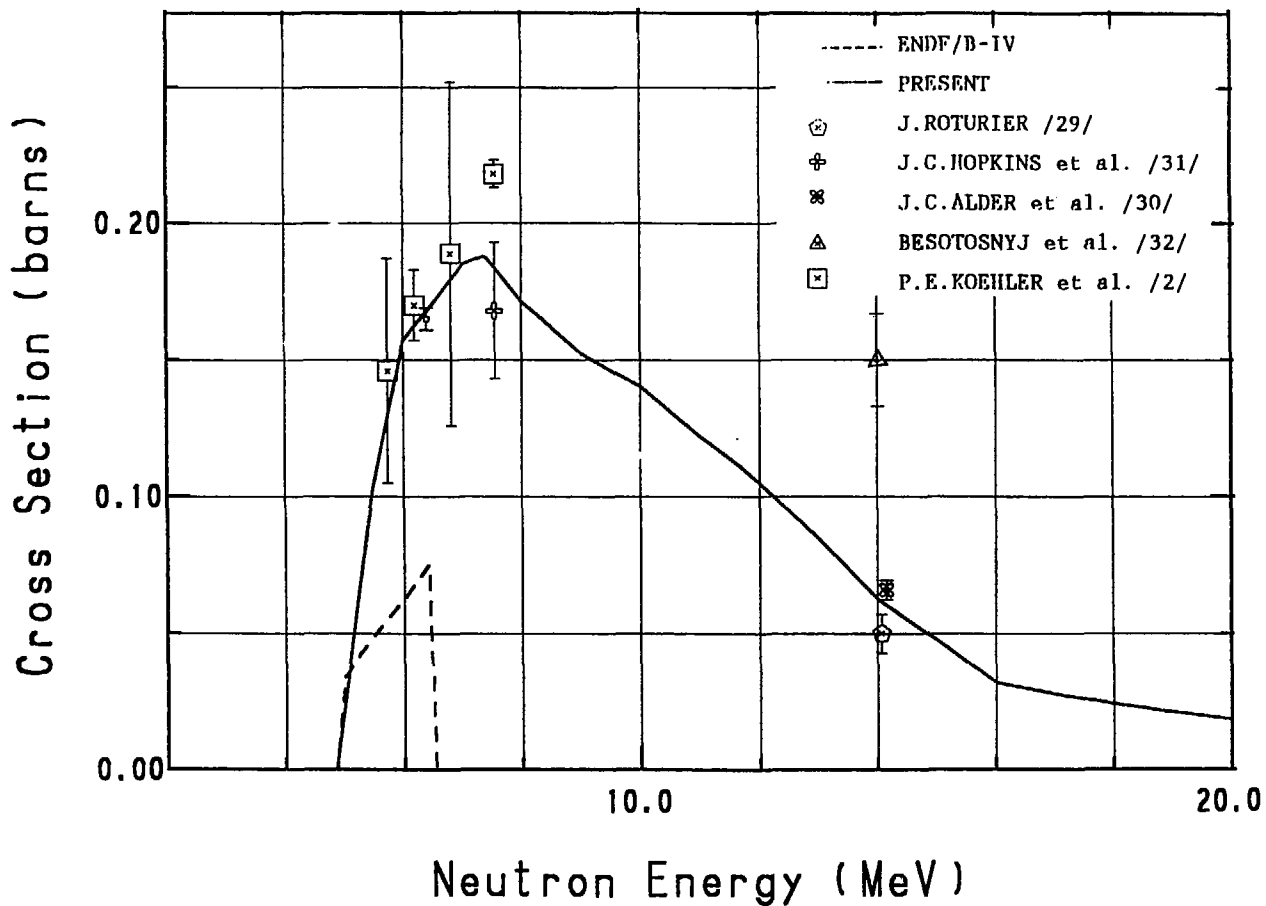


Fig.5 (b) Inelastic Scattering Cross Sections of the Second Excited Level ($Q=-4.45$ MeV)

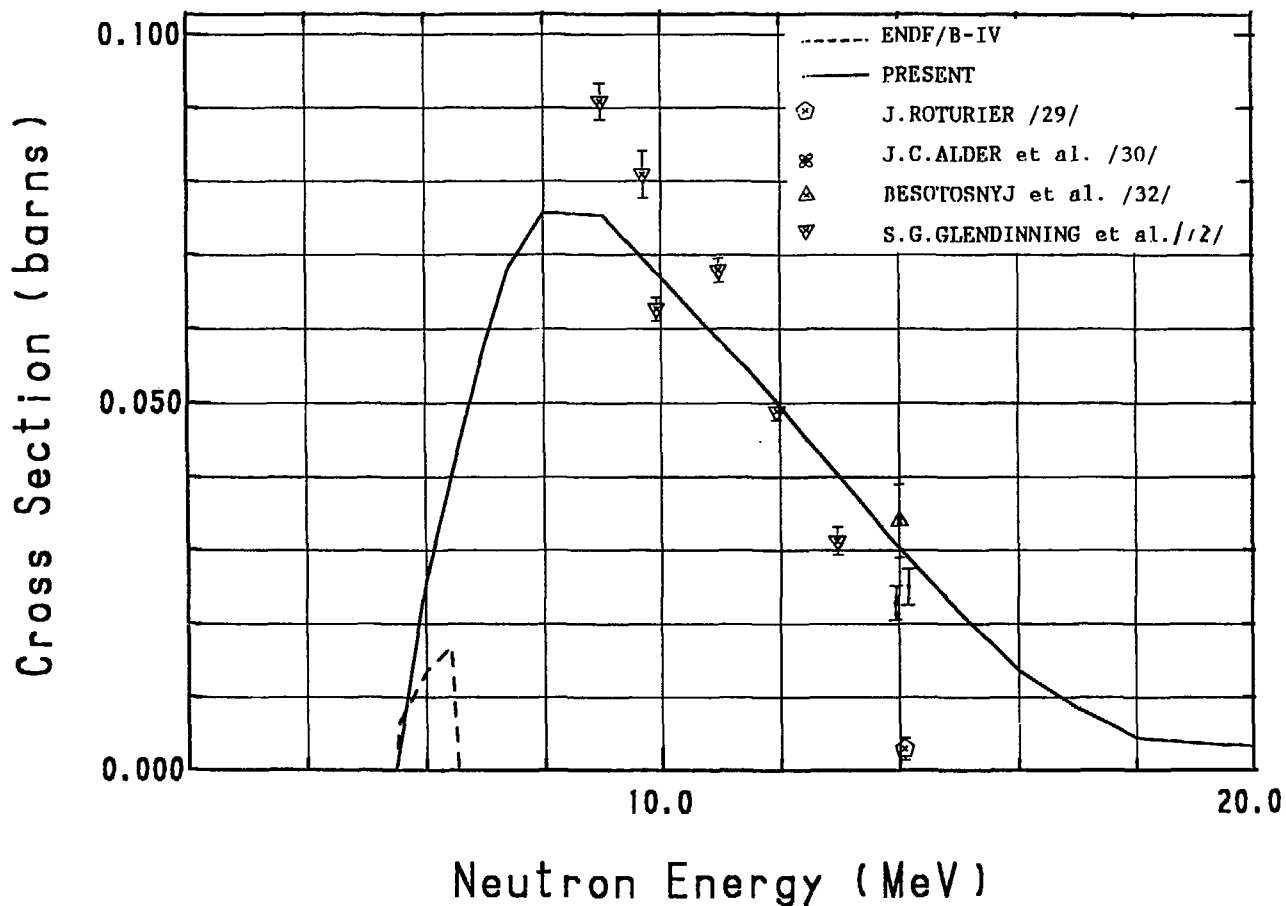


Fig.5 (c) Inelastic Scattering Cross Sections of the Third Excited Level ($Q=-5.02$ MeV)

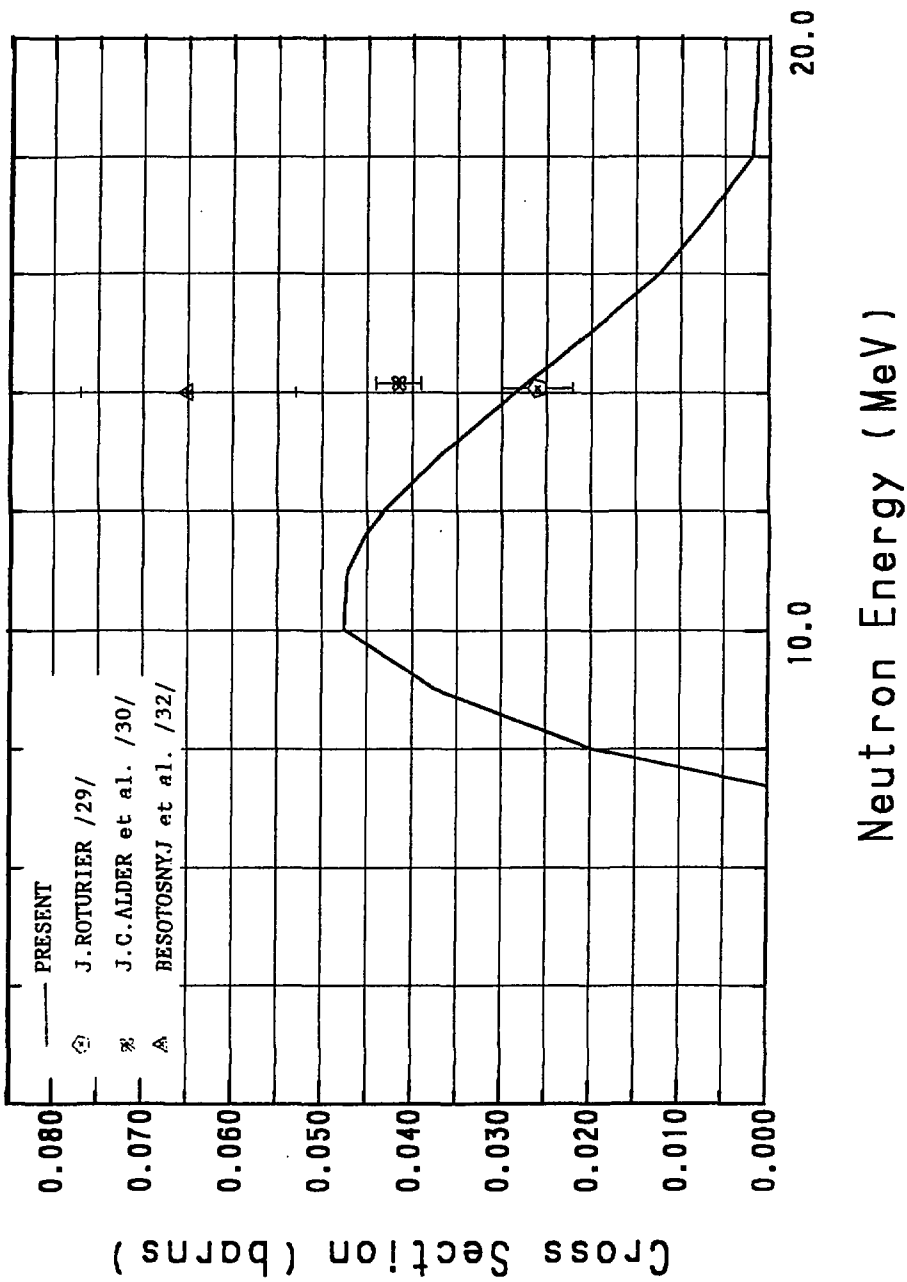


Fig. 5 (d) Inelastic Scattering Cross Sections of the Fourth Excited Level ($Q=-6.74$ MeV)

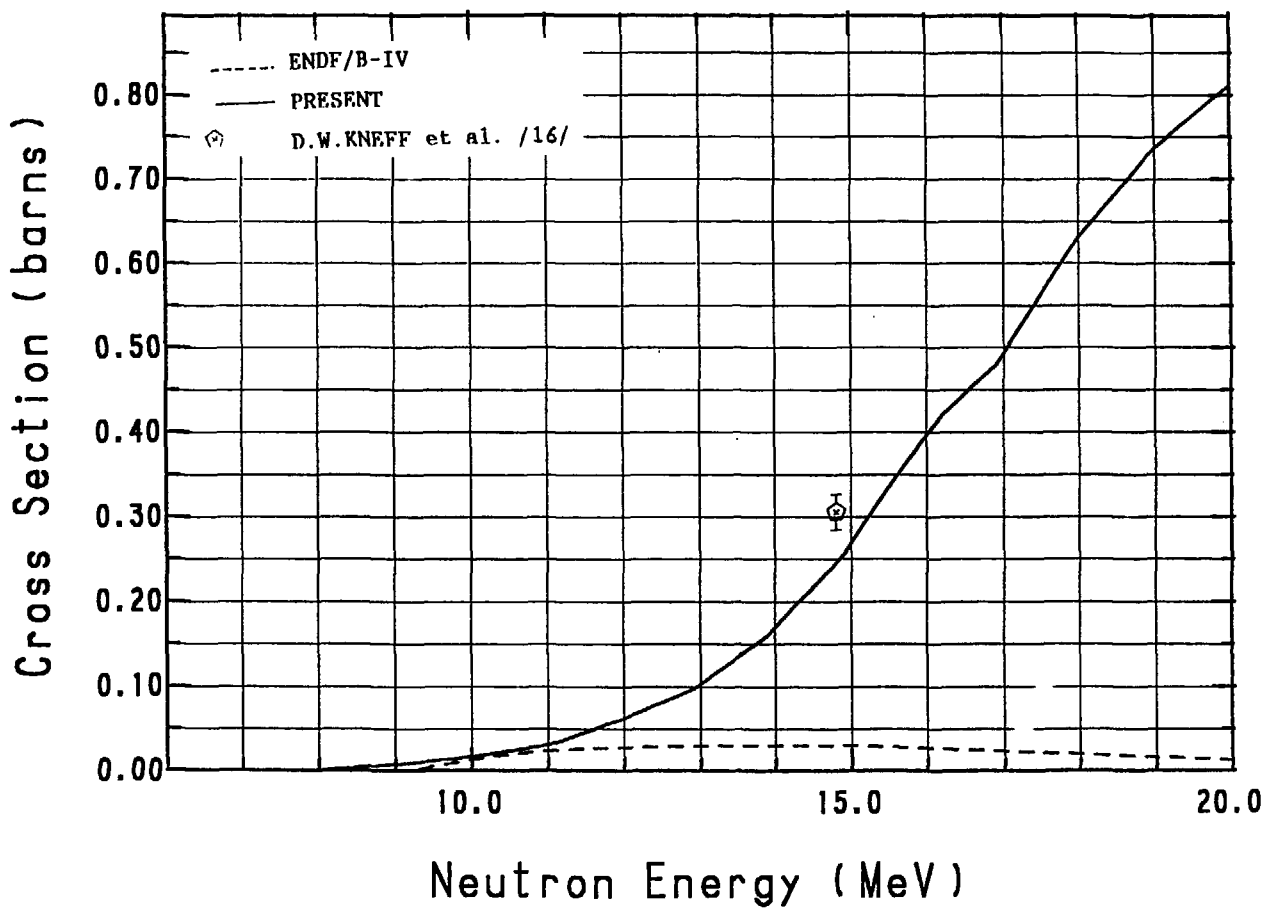


Fig.6 Helium Production Cross Section

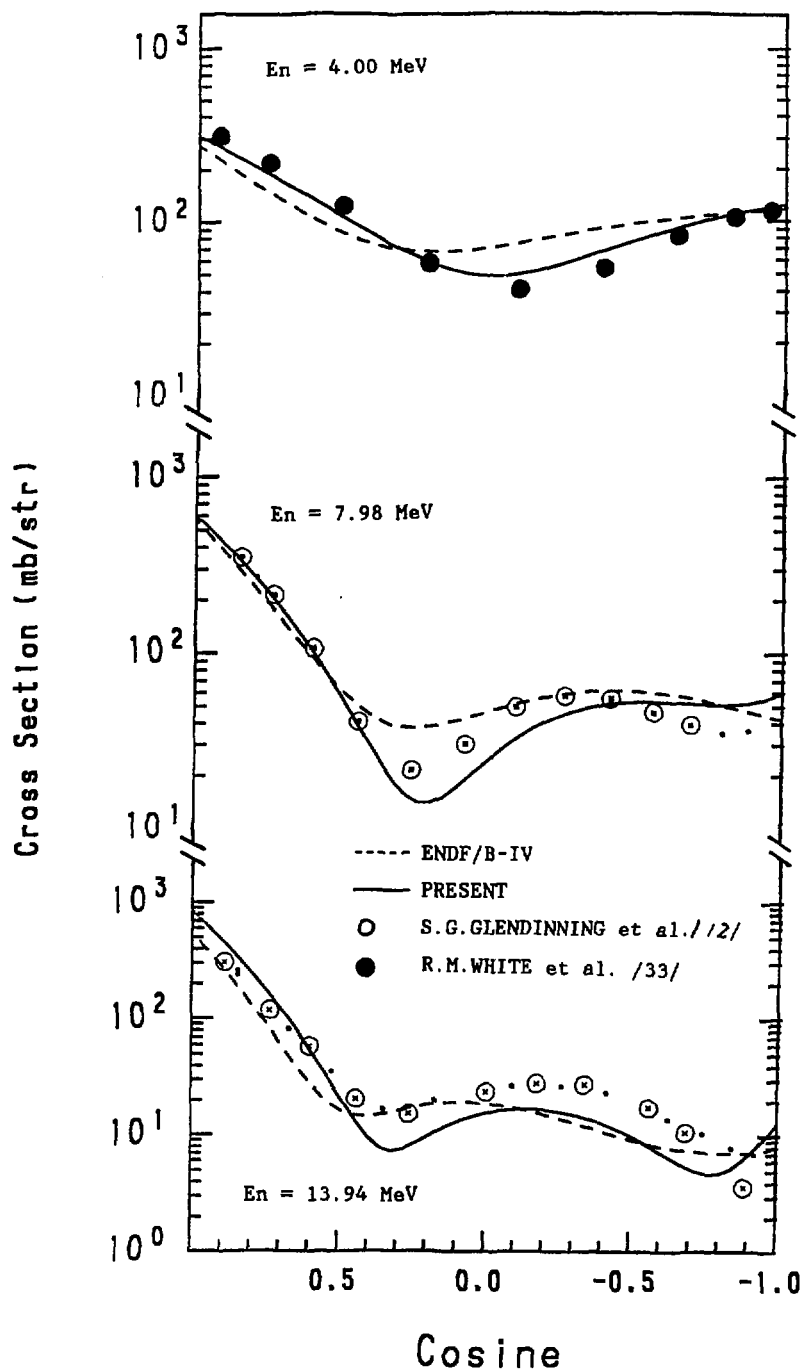


Fig. 7 Angular Distributions of Elastic Scattering

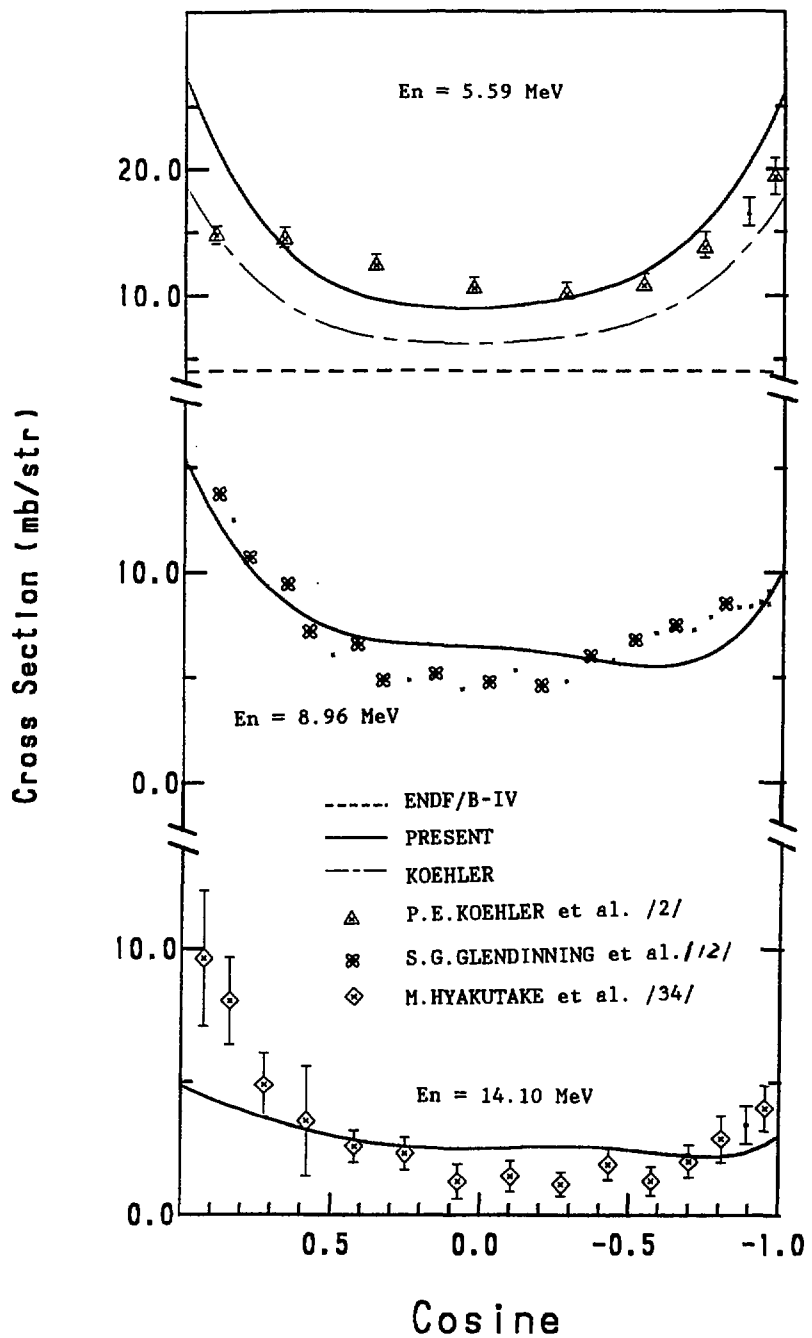


Fig. 8 (a) Angular Distributions of Inelastic Scattering of the First Excited Level ($Q=-2.12$ MeV)

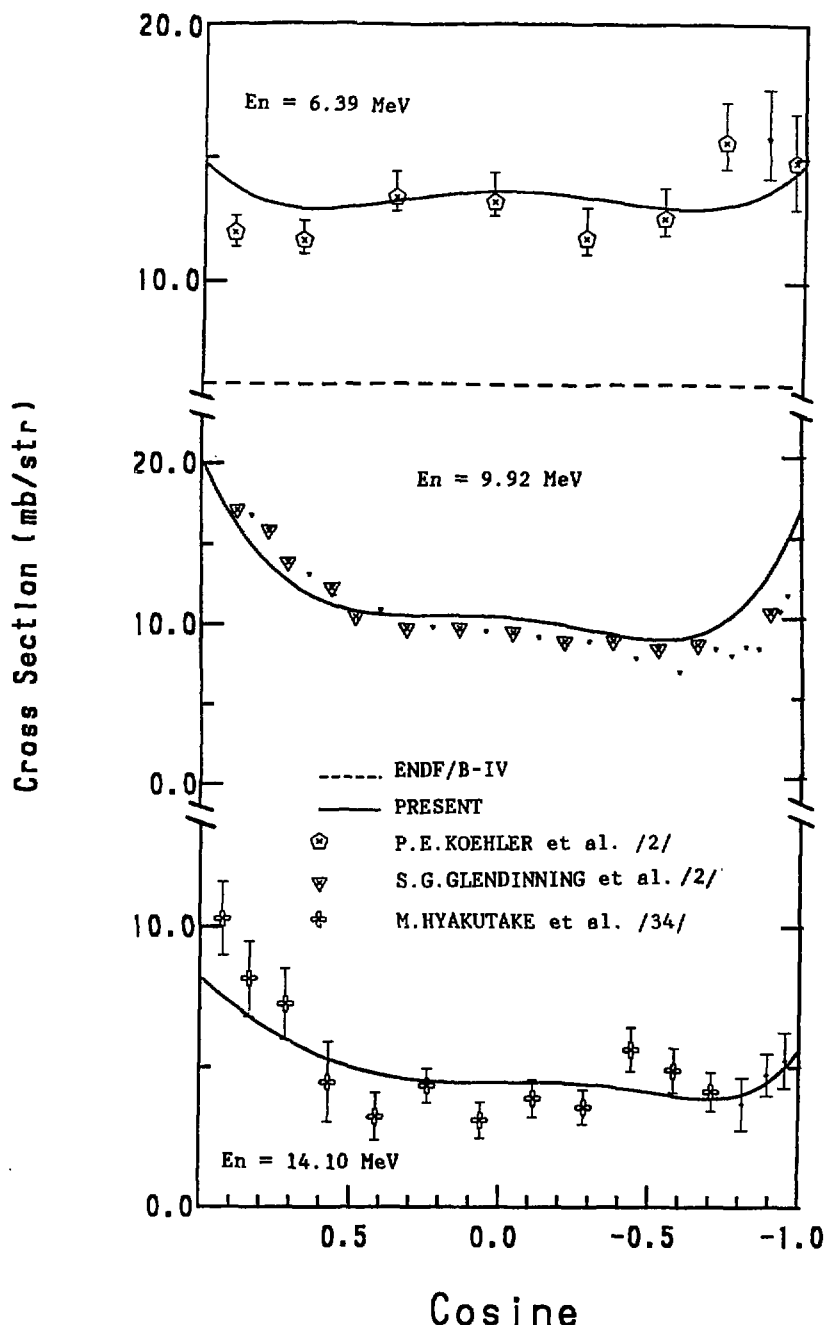


Fig. 8 (b) Angular Distributions of Inelastic Scattering of the Second Excited Level ($Q=-4.45 \text{ MeV}$)

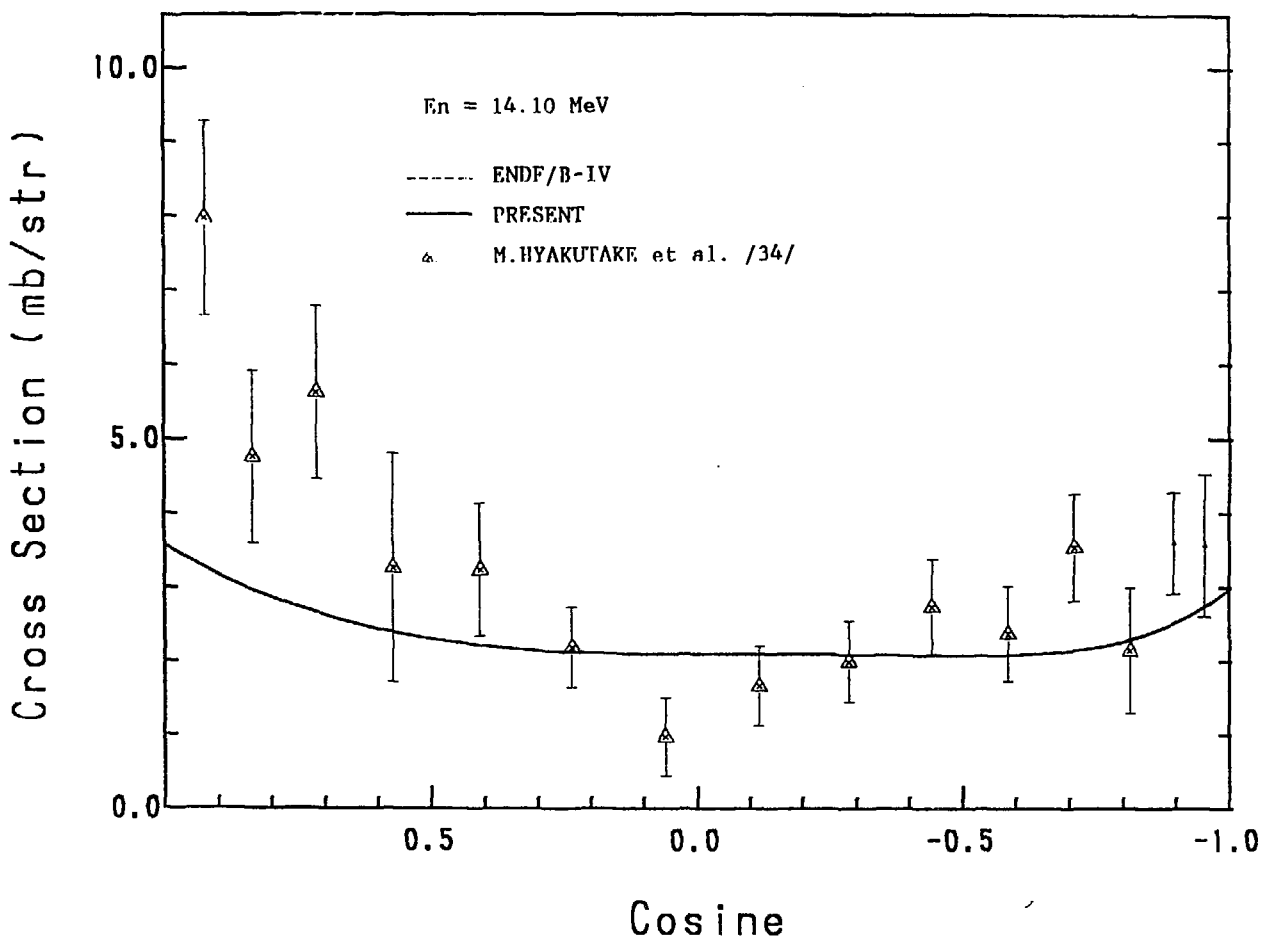


Fig.8 (c) Angular Distributions of Inelastic Scattering of the Third Excited Level ($Q=-5.02$ MeV)

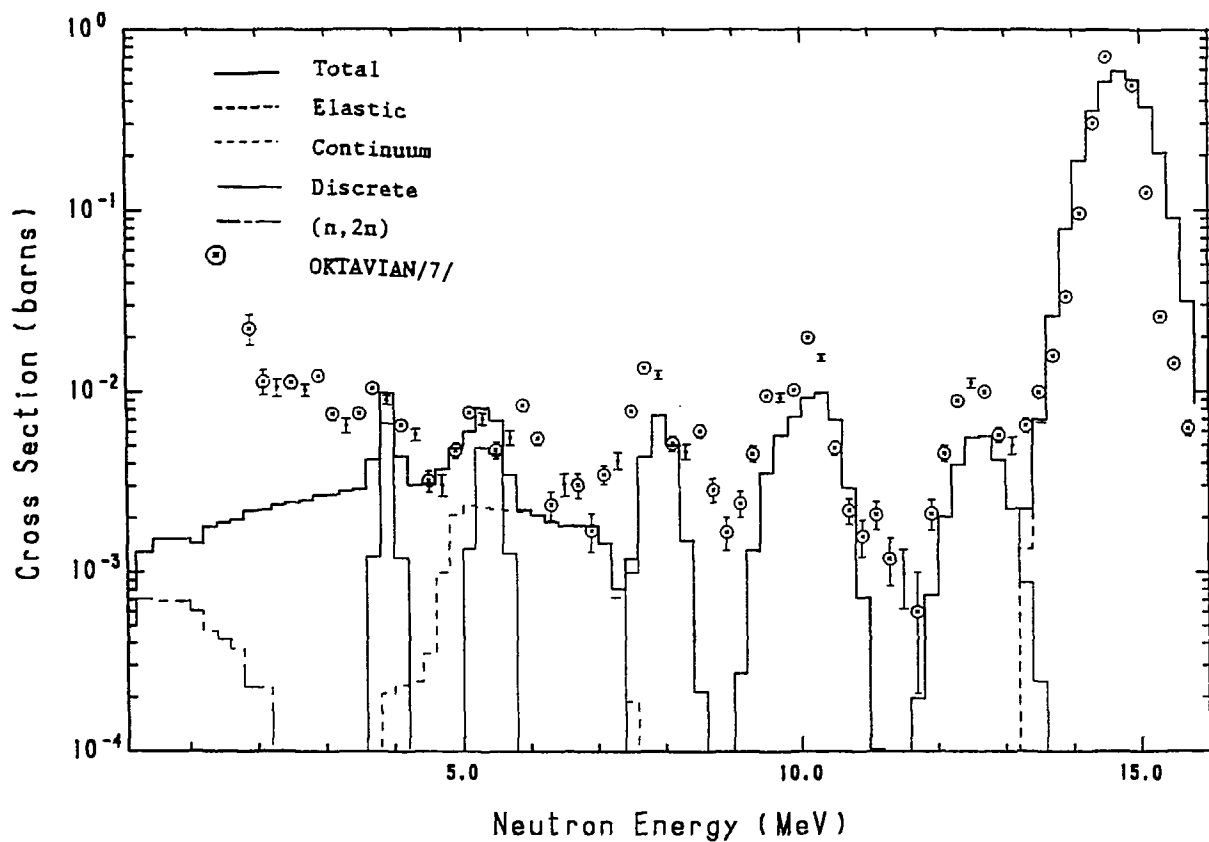


Fig.9 (a) Double Differential Cross Section Compared with the
Experimental Data of OKTAVIAN/7/ (14.83 MeV, 20 deg.)

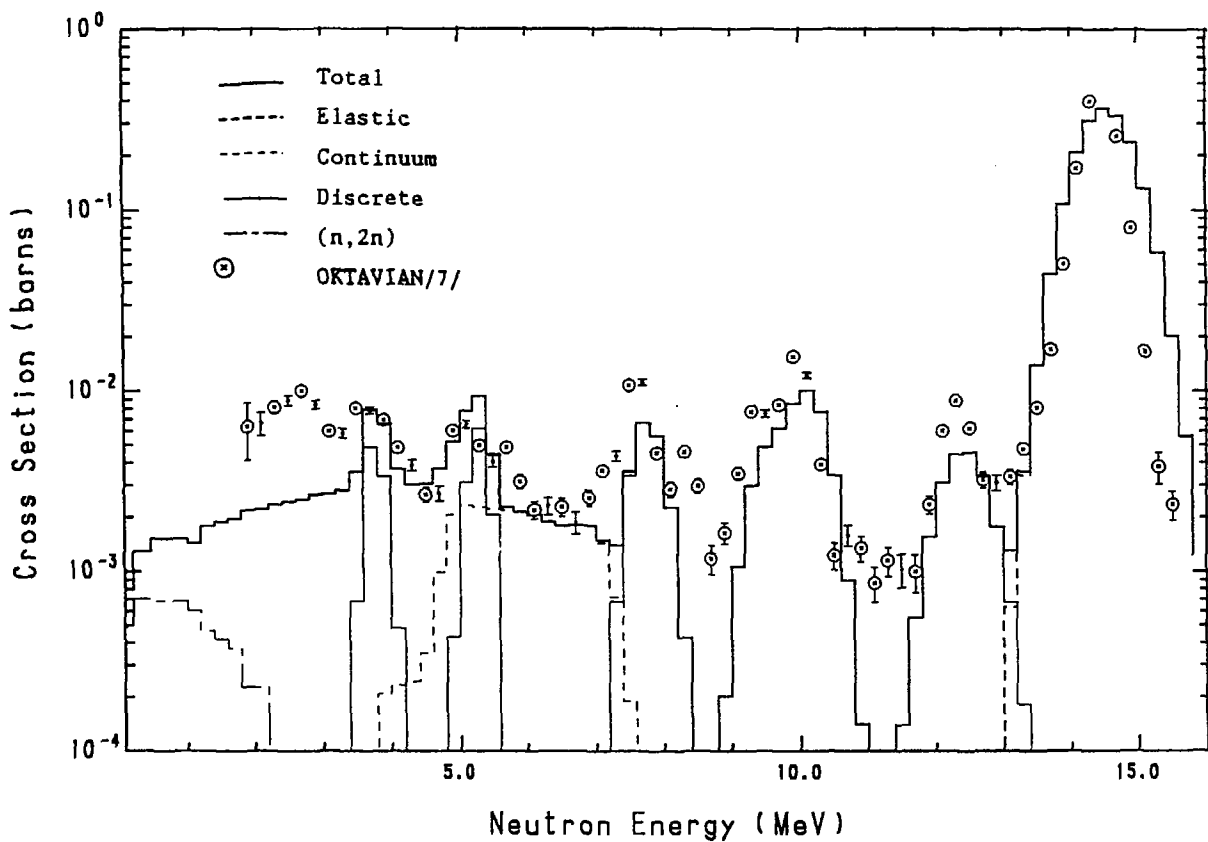


Fig.9 (b) Double Differential Cross Section Compared with the Experimental Data of OKTAVIAN/7/ (14.80 MeV, 30 deg.)

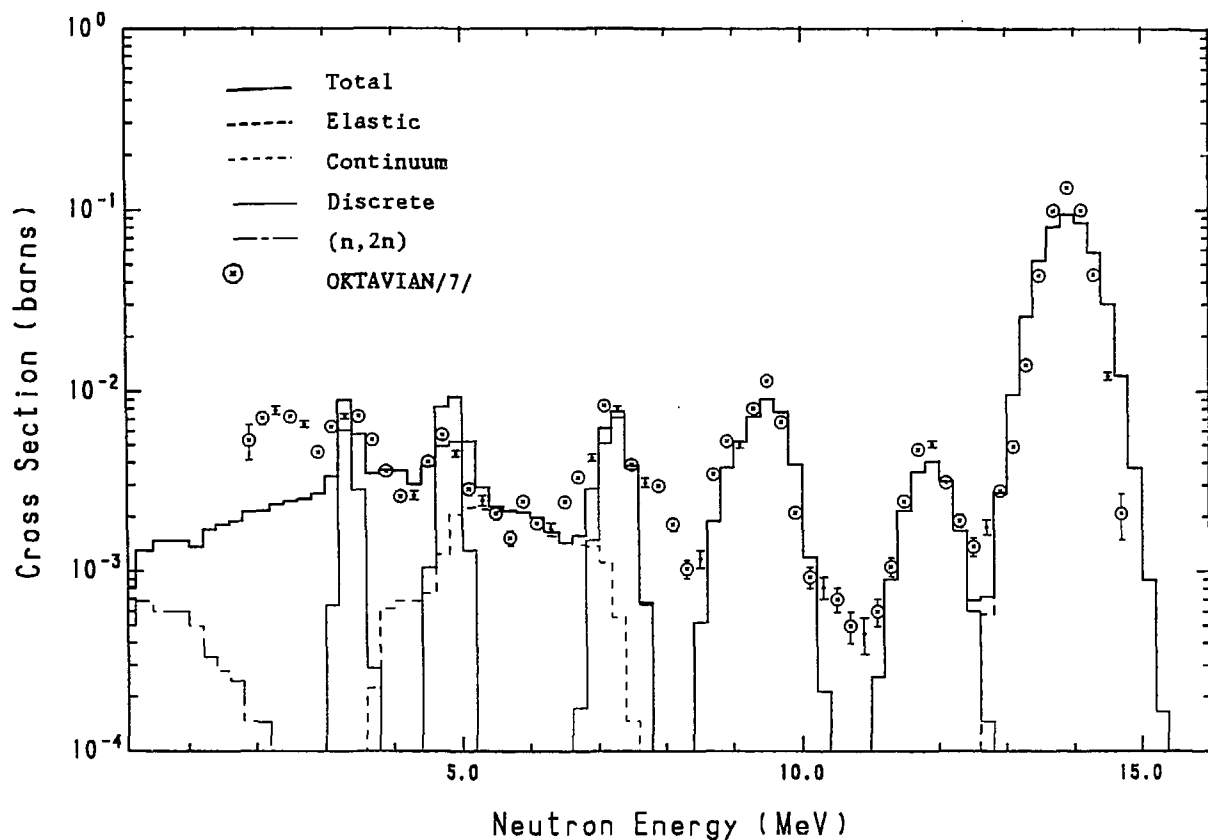


Fig.9 (c) Double Differential Cross Section Compared with the
Experimental Data of OKTAVIAN/7/ (14.67 MeV, 45 deg.)

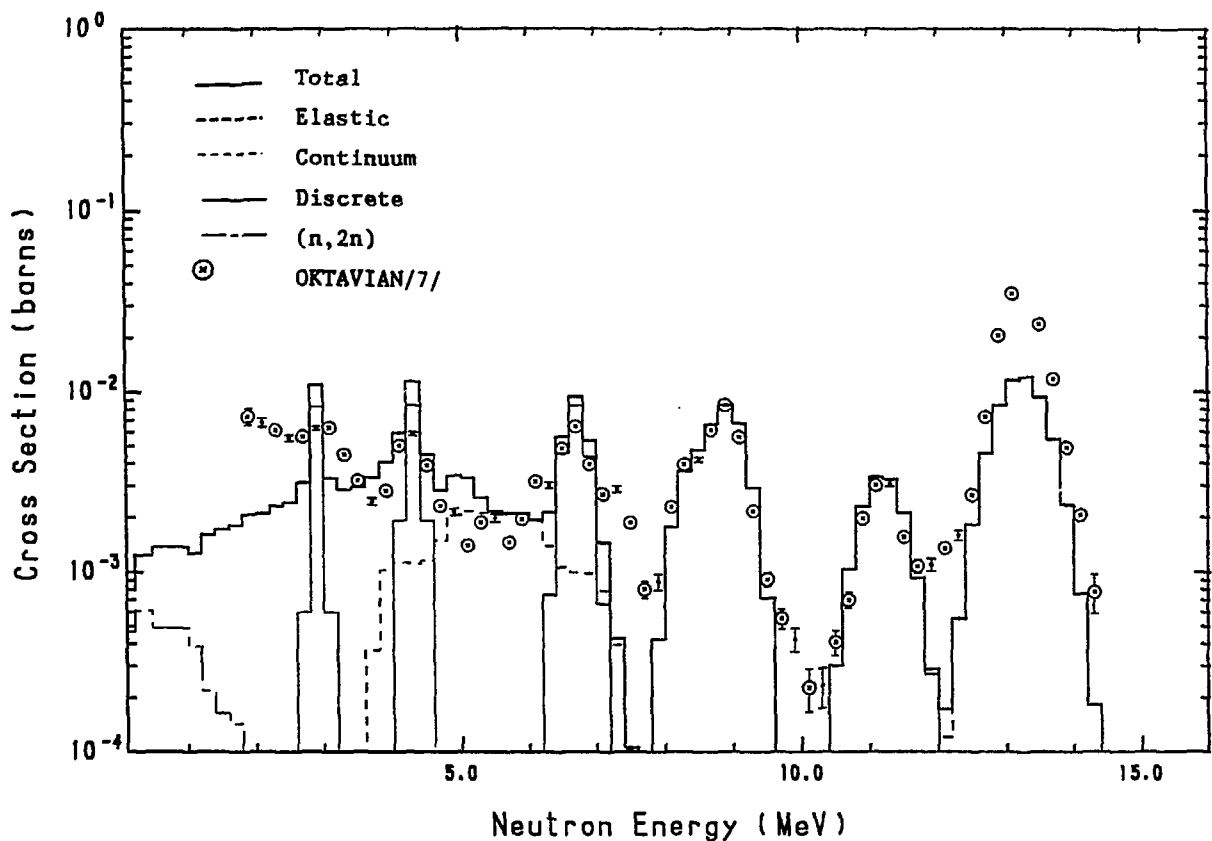


Fig.9 (d) Double Differential Cross Section Compared with the Experimental Data of OKTAVIAN/7/ (14.53 MeV, 60 deg.)

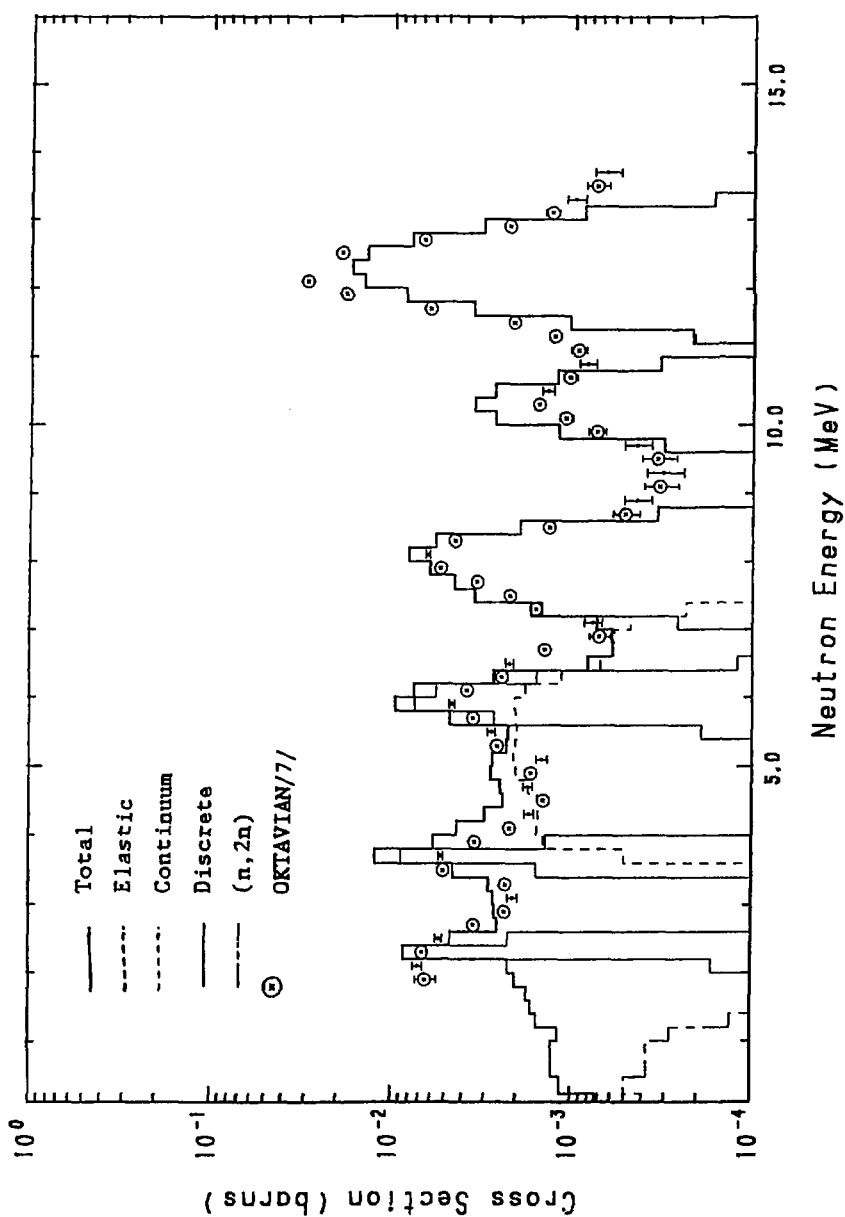


Fig. 9 (e) Double Differential Gross Section Compared with the Experimental Data of OKTAVIAN/7/ (14.25 MeV, 80 deg.)

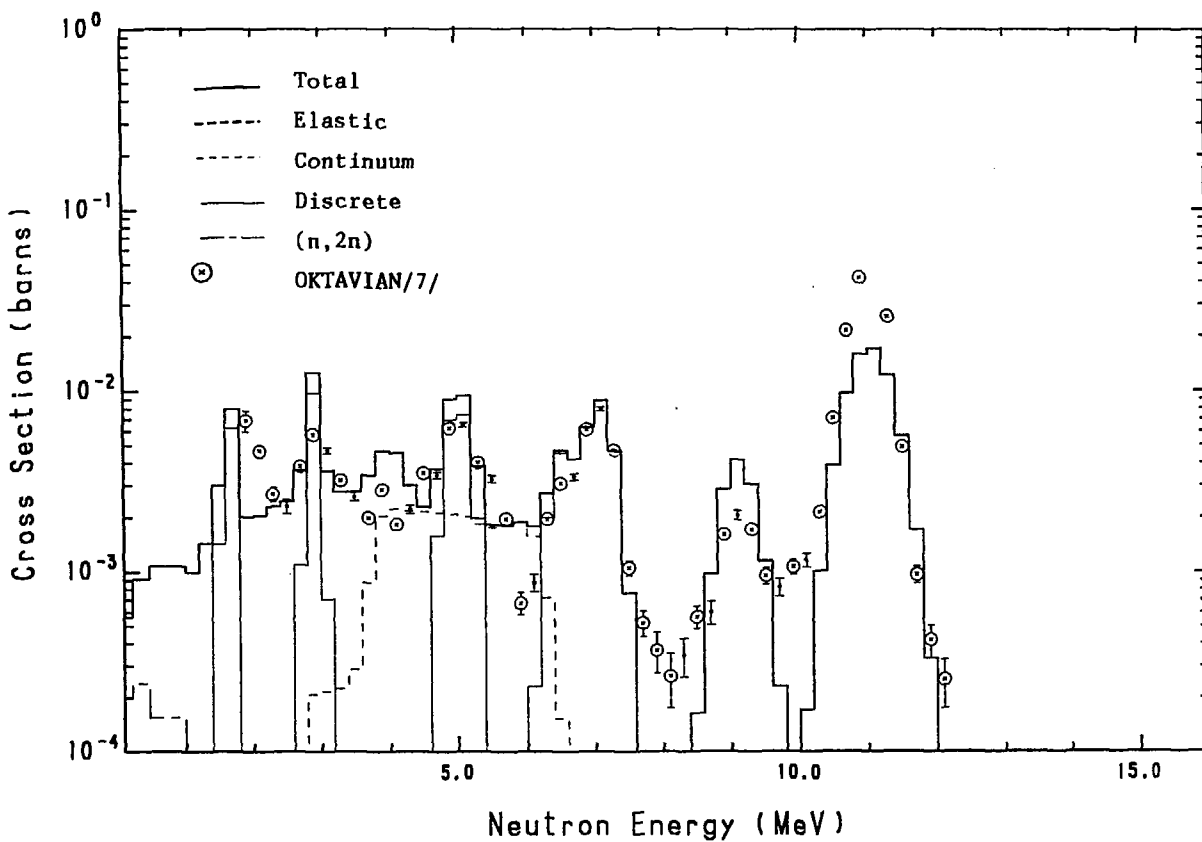


Fig. 9 (f) Double Differential Cross Section Compared with the Experimental Data of OKTAVIAN/7/ (13.95 MeV, 105 deg.)

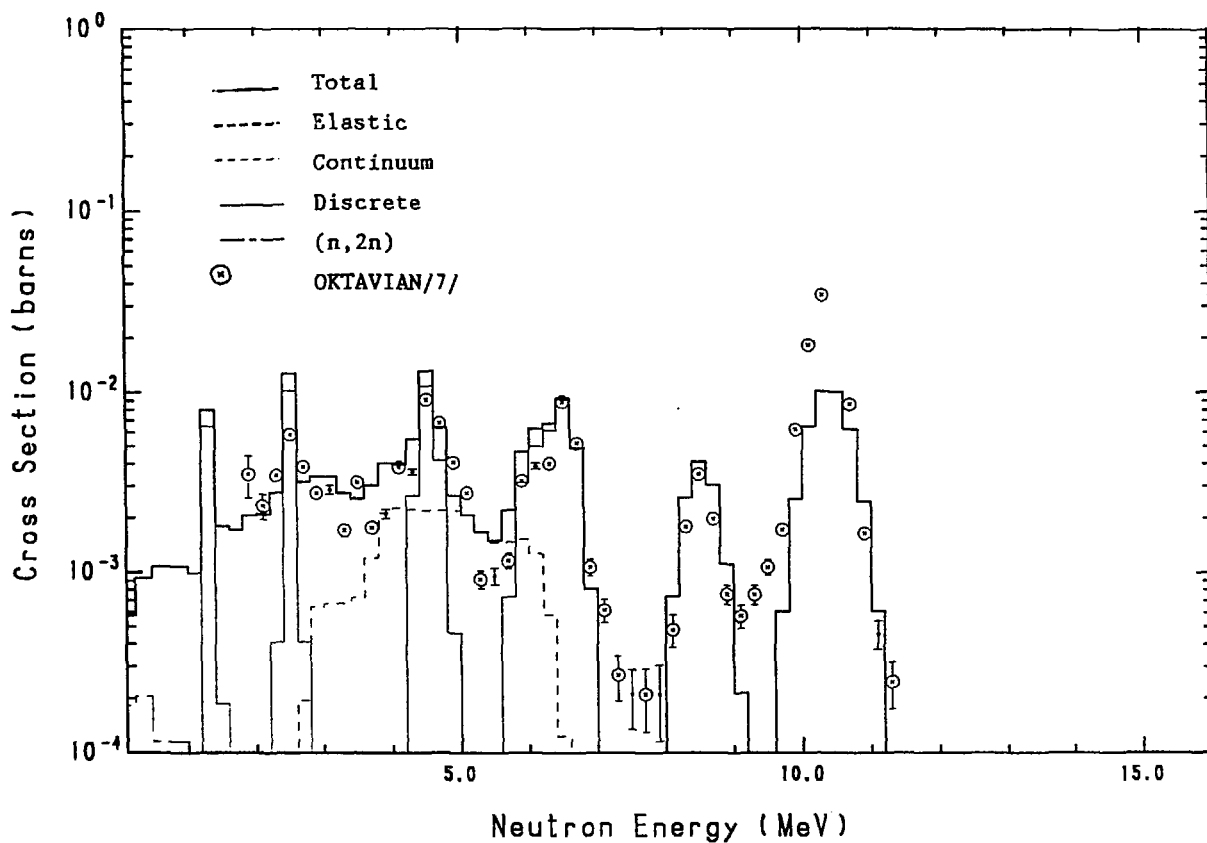


Fig. 9 (g) Double Differential Cross Section Compared with the
Experimental Data of OKTAVIAN/7/ (13.74 MeV, 120 deg.)

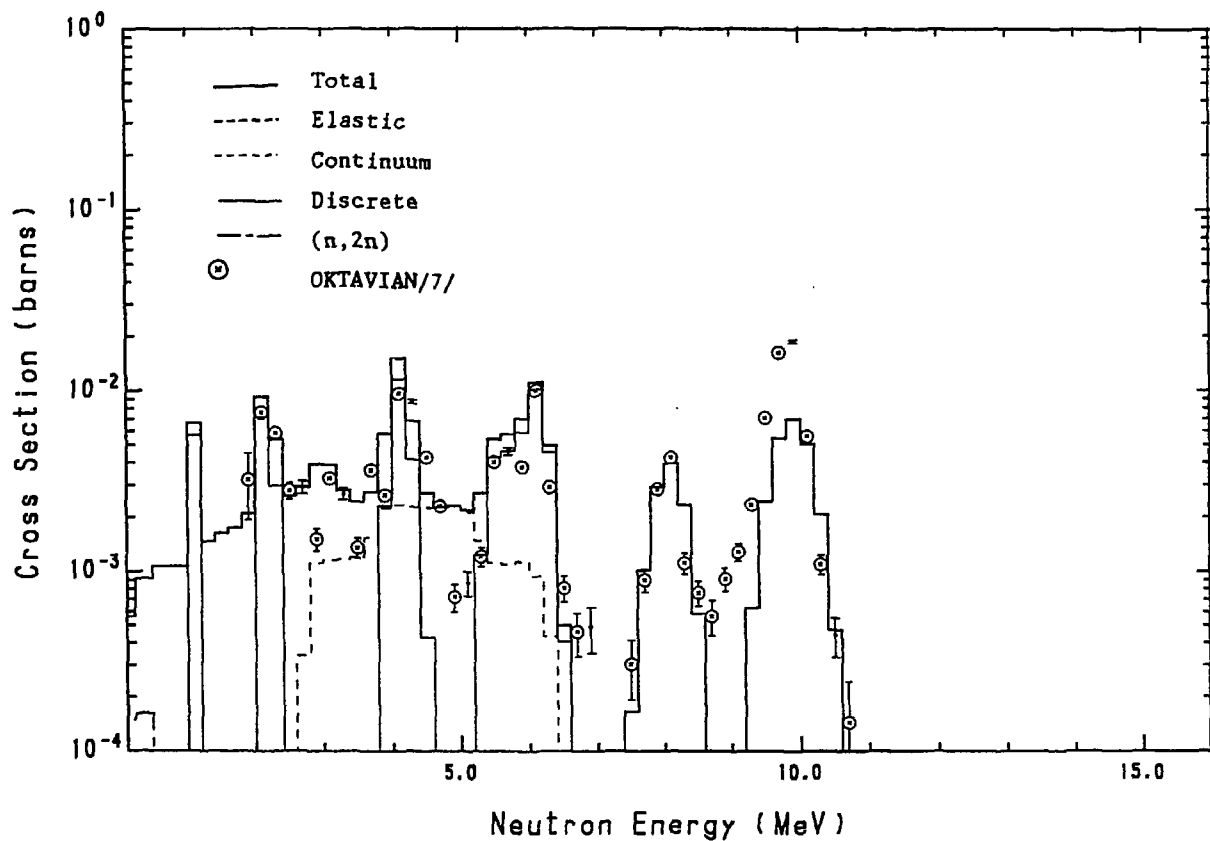


Fig.9 (h) Double Differential Cross Section Compared with the Experimental Data of OKTAVIAN/7/ (13.56 MeV, 135 deg.)

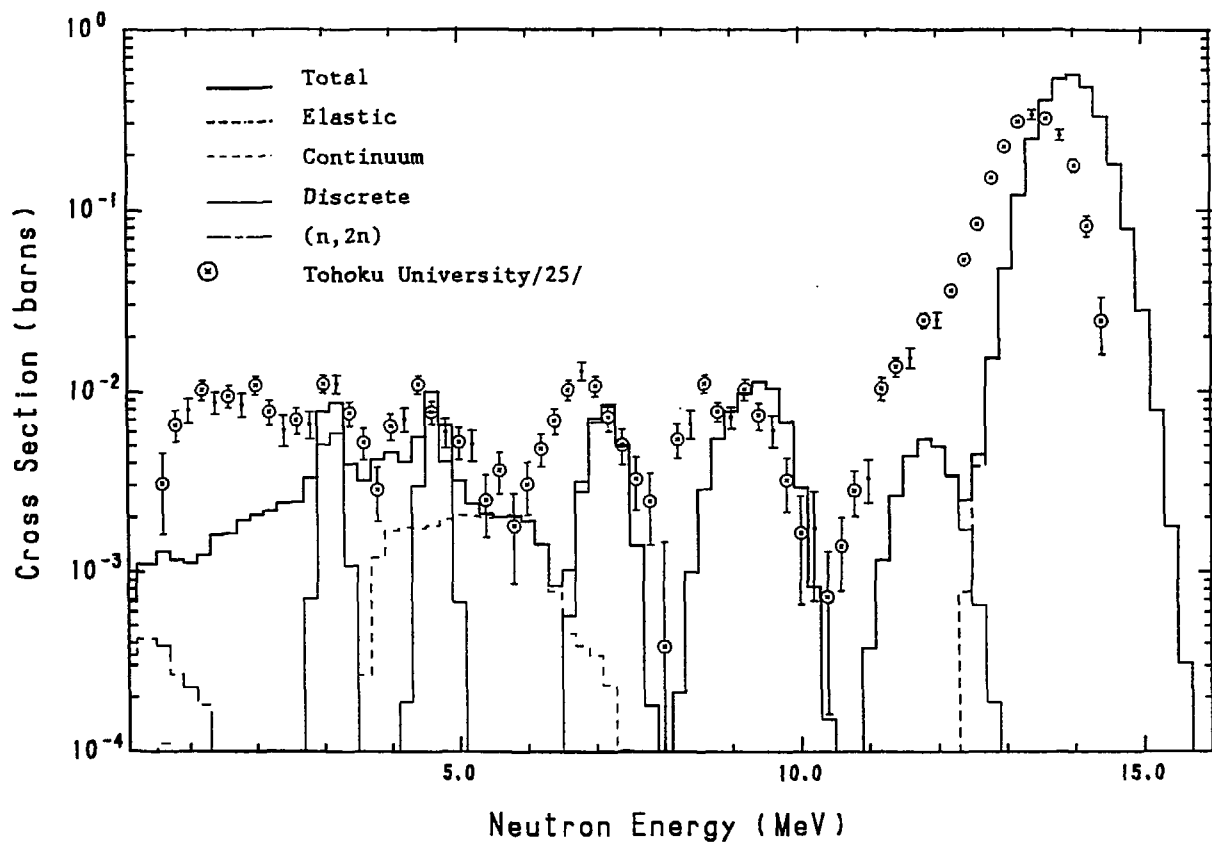


Fig.10 (a) Double Differential Cross Section Compared with the
Experimental Data of Tohoku University/25/ (14.2 MeV, 25 deg.)

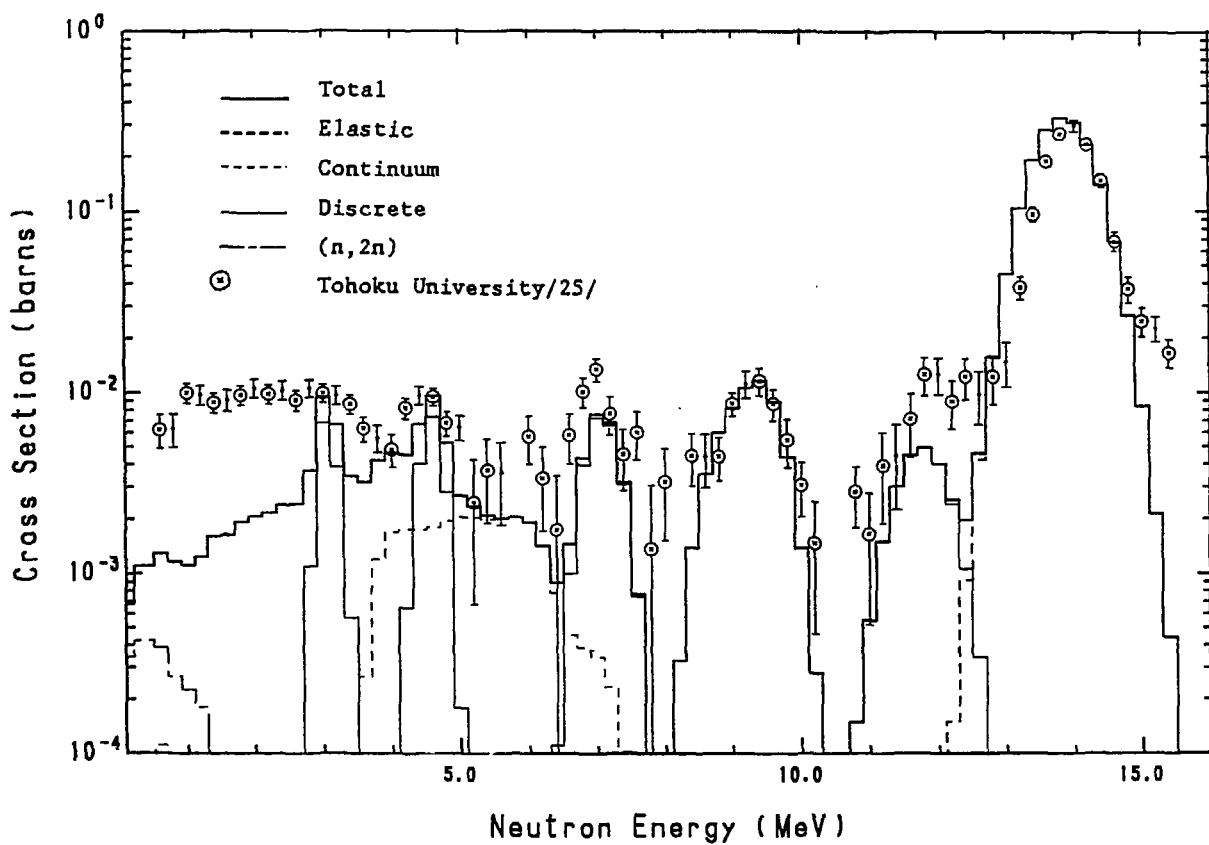


Fig. 10 (b) Double Differential Cross Section Compared with the Experimental Data of Tohoku University/25/ (14.2 MeV, 30 deg.)

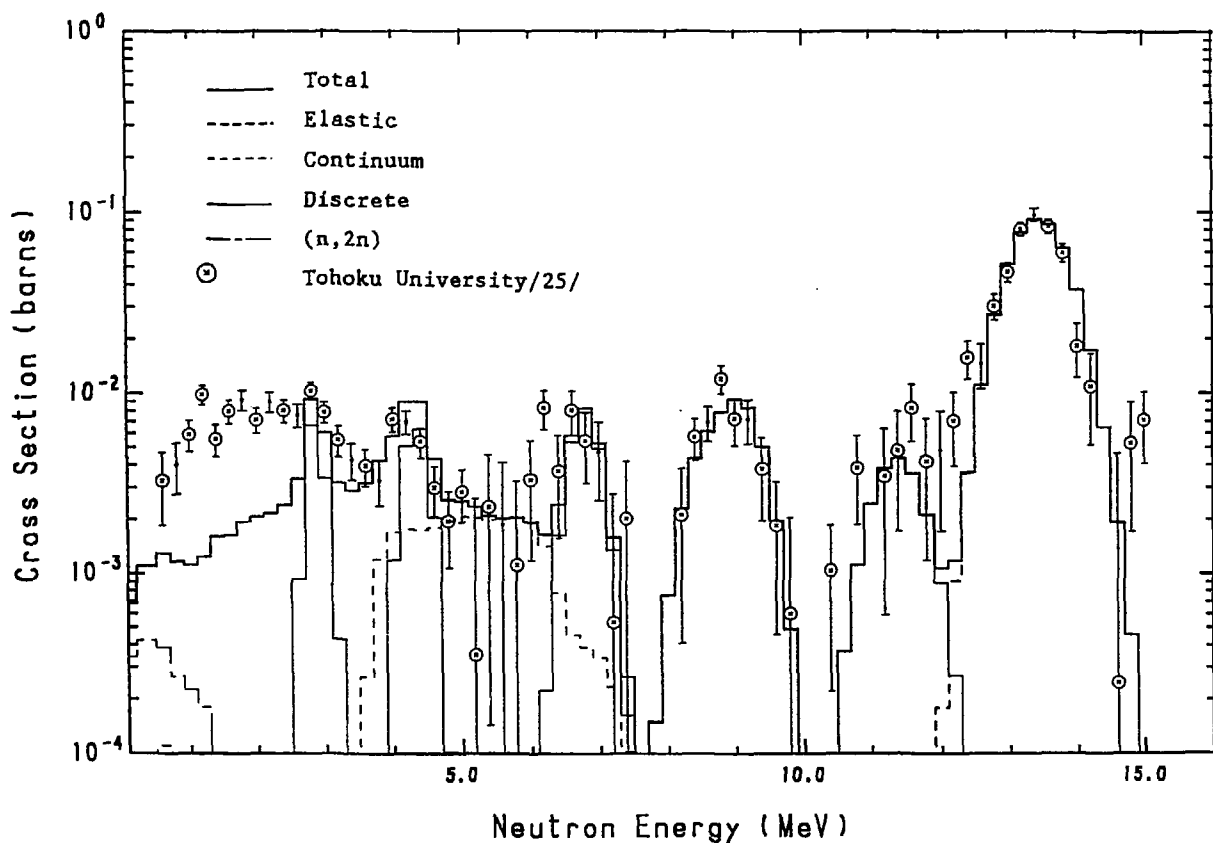


Fig.10 (c) Double Differential Cross Section Compared with the
Experimental Data of Tohoku University/25/ (14.2 MeV, 45 deg.)

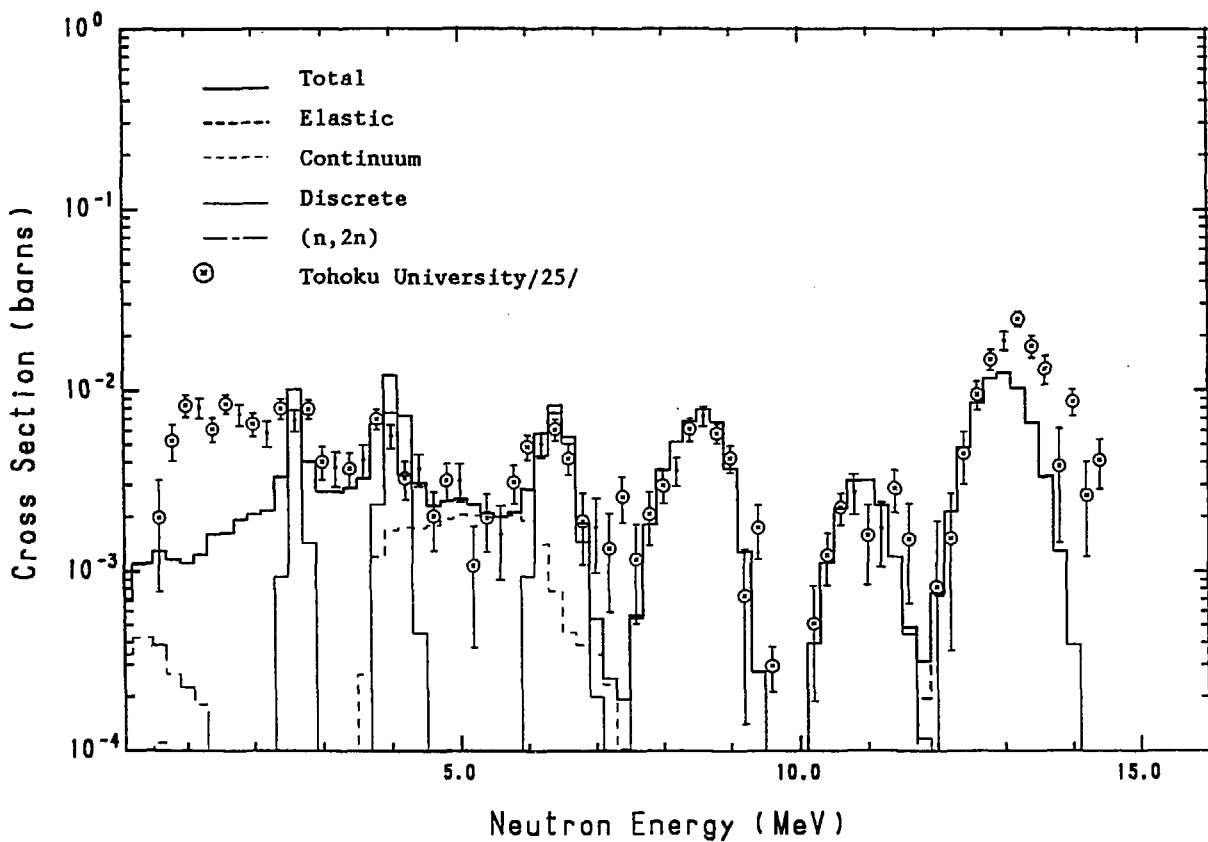


Fig.10 (d) Double Differential Cross Section Compared with the
Experimental Data of Tohoku University/25/ (14.2 MeV, 60 deg.)

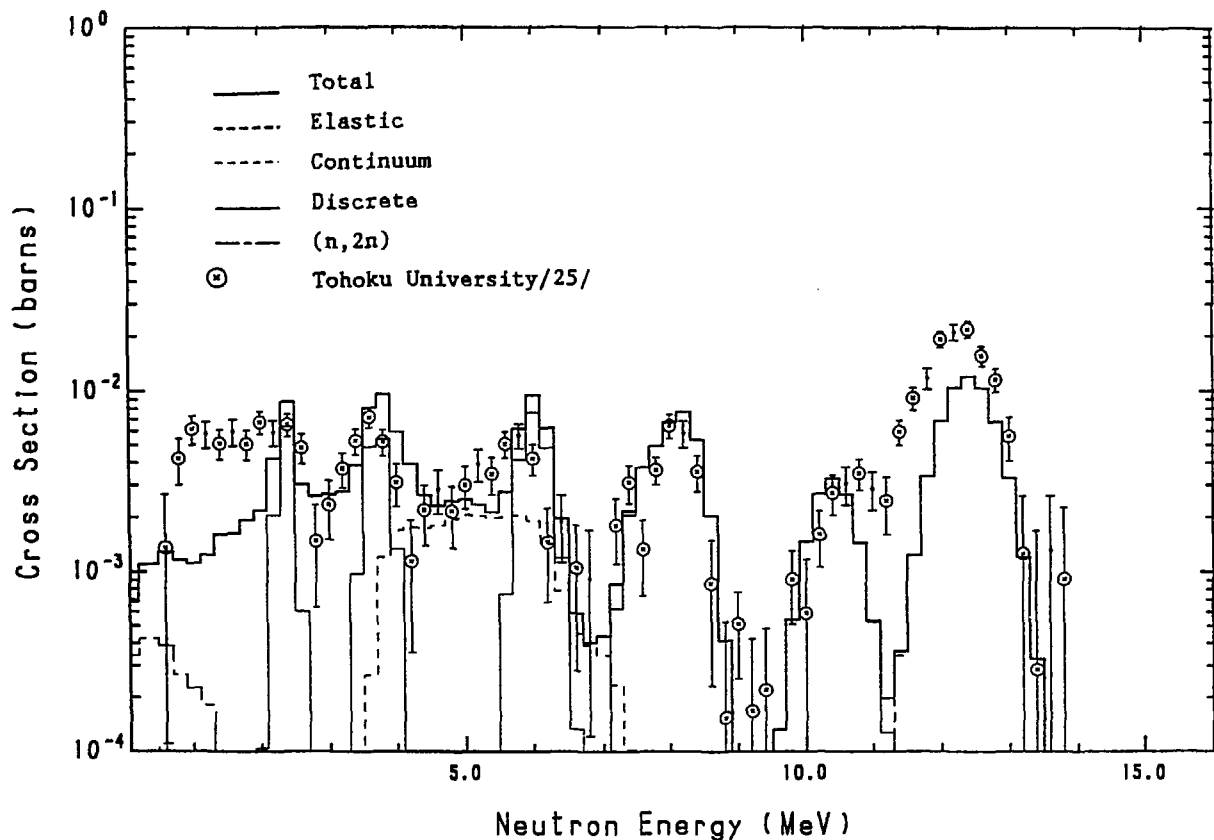


Fig.10 (e) Double Differential Cross Section Compared with the
 Experimental Data of Tohoku University/25/ (14.2 MeV, 75 deg.)

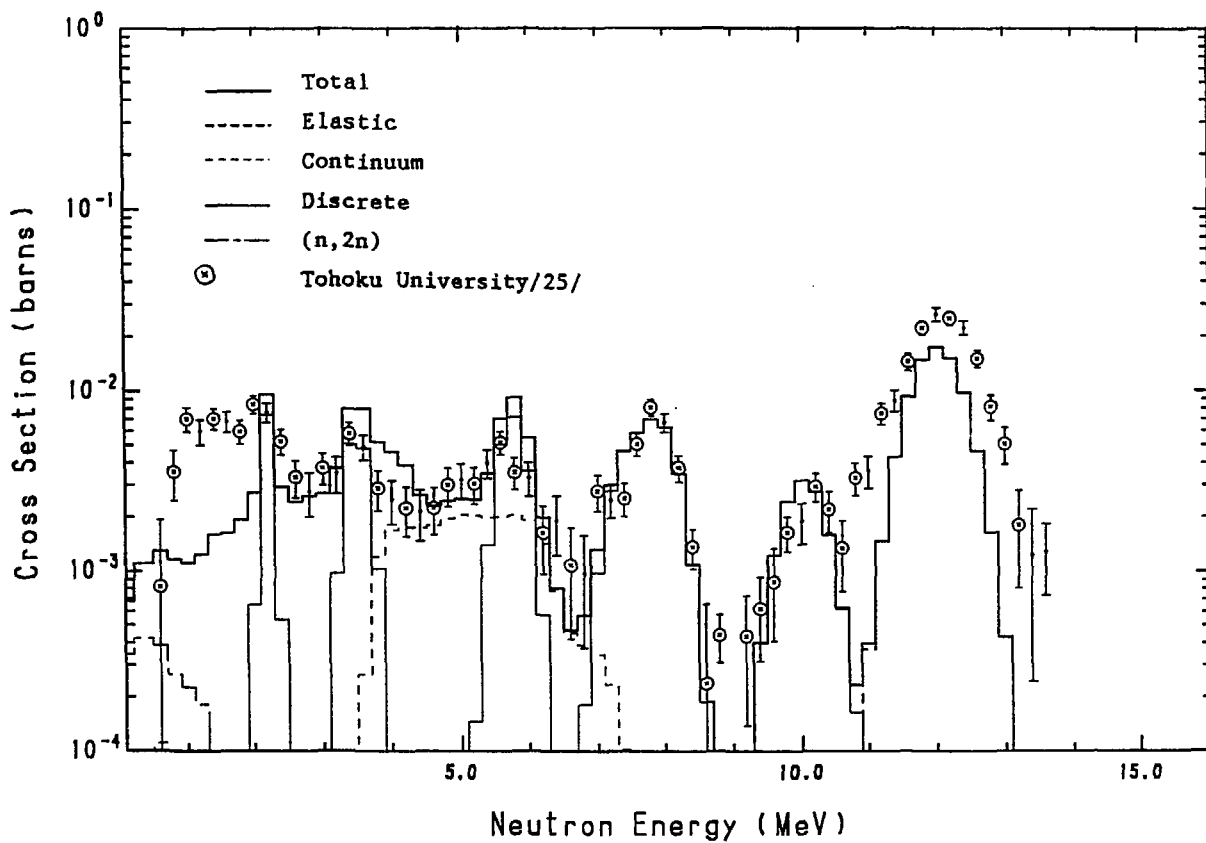


Fig.10 (f) Double Differential Cross Section Compared with the
Experimental Data of Tohoku University/25/ (14.2 MeV, 85 deg.)

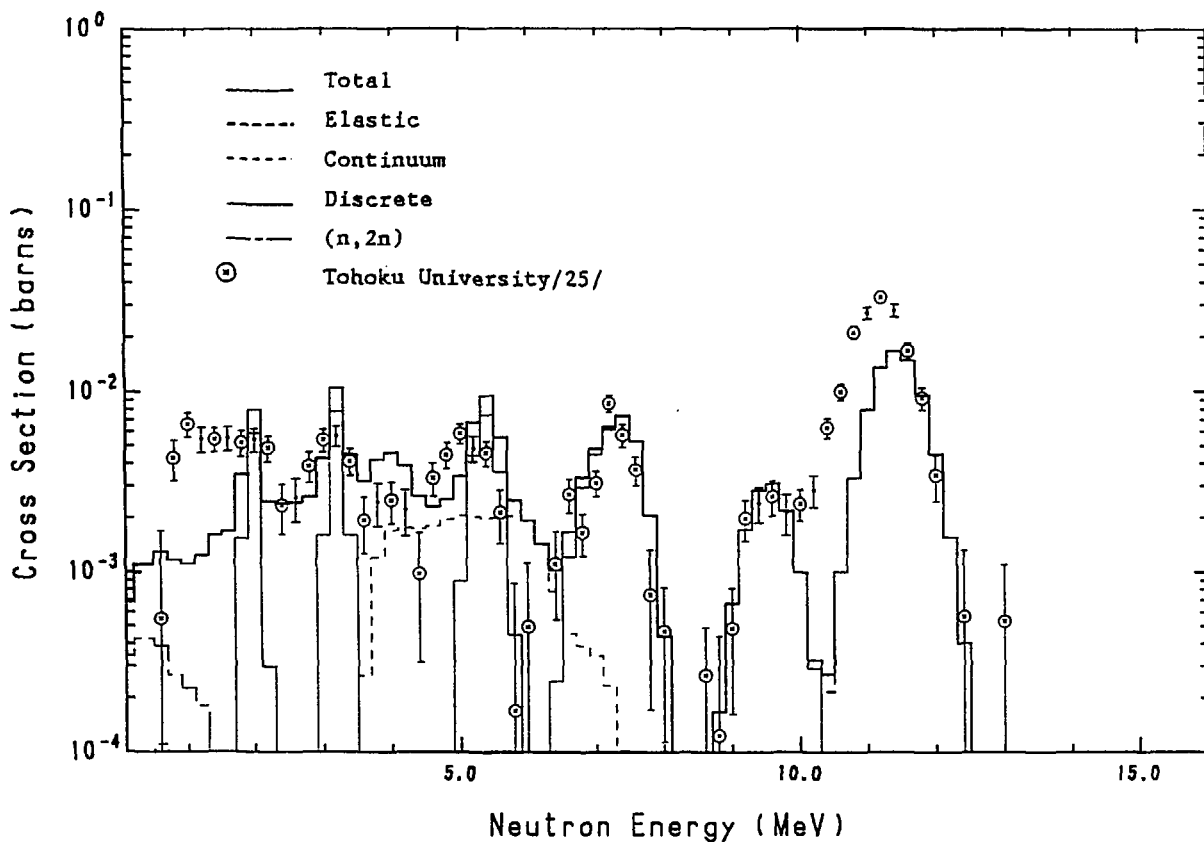


Fig.10 (g) Double Differential Cross Section Compared with the
Experimental Data of Tohoku University/25/ (14.2 MeV, 100 deg.)

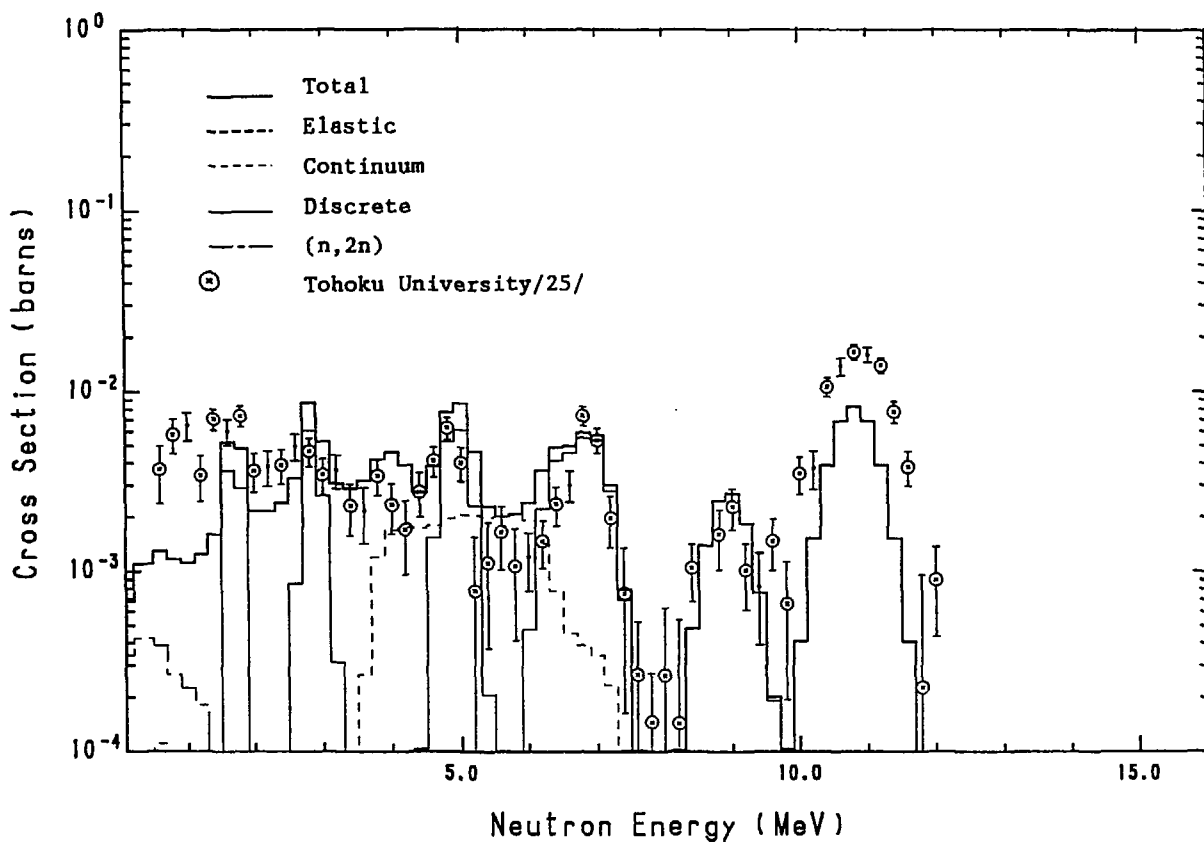


Fig.10 (h) Double Differential Cross Section Compared with the
Experimental Data of Tohoku University/25/ (14.2 MeV, 120 deg.)

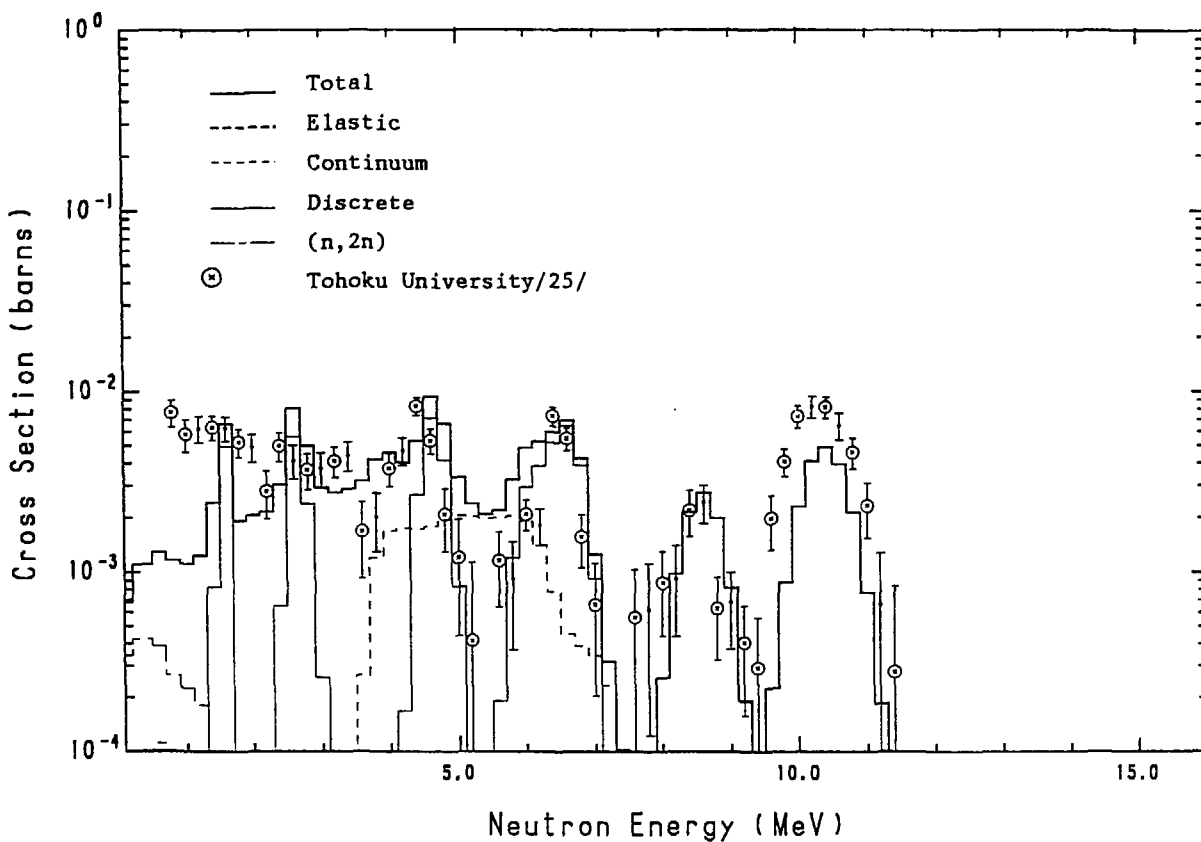


Fig.10 (i) Double Differential Cross Section Compared with the
Experimental Data of Tohoku University/25/ (14.2 MeV, 135 deg.)

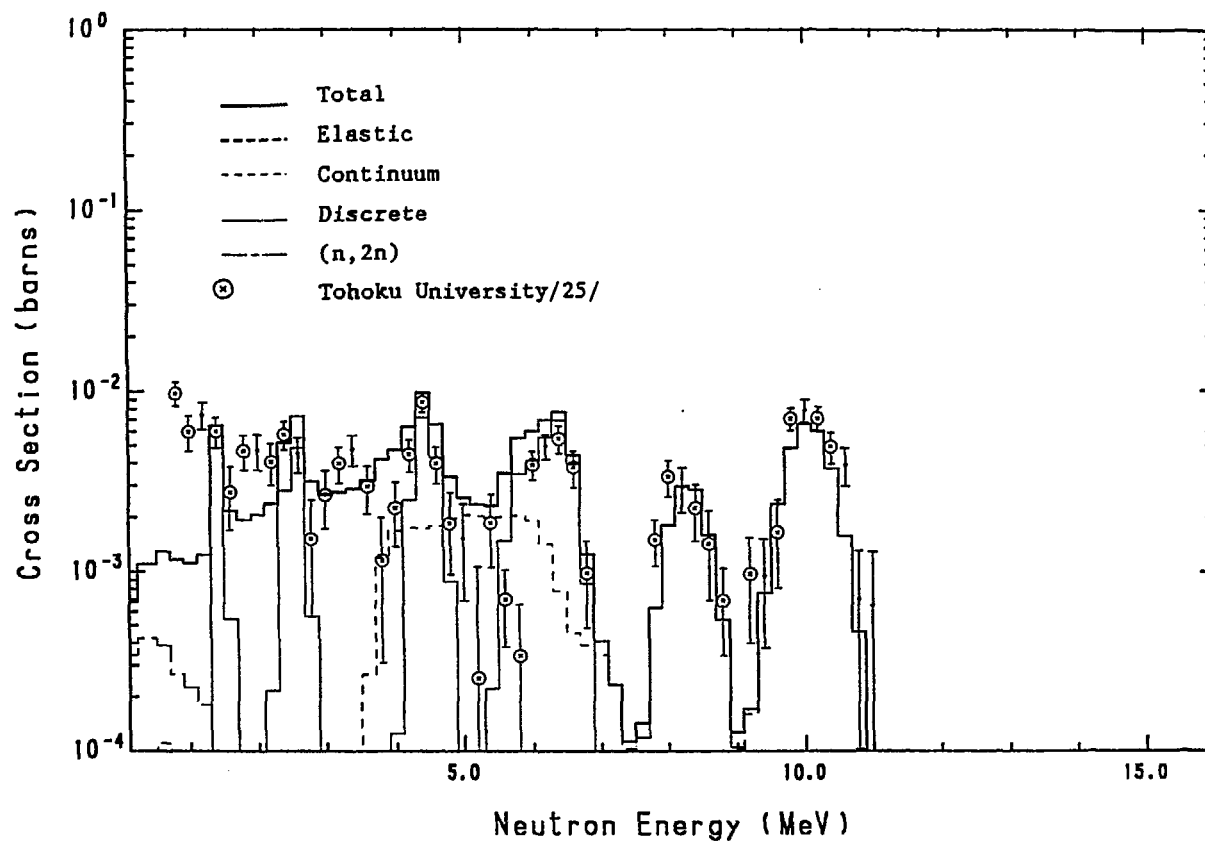


Fig.10 (j) Double Differential Cross Section Compared with the
Experimental Data of Tohoku University/25/ (14.2 MeV, 150 deg.)

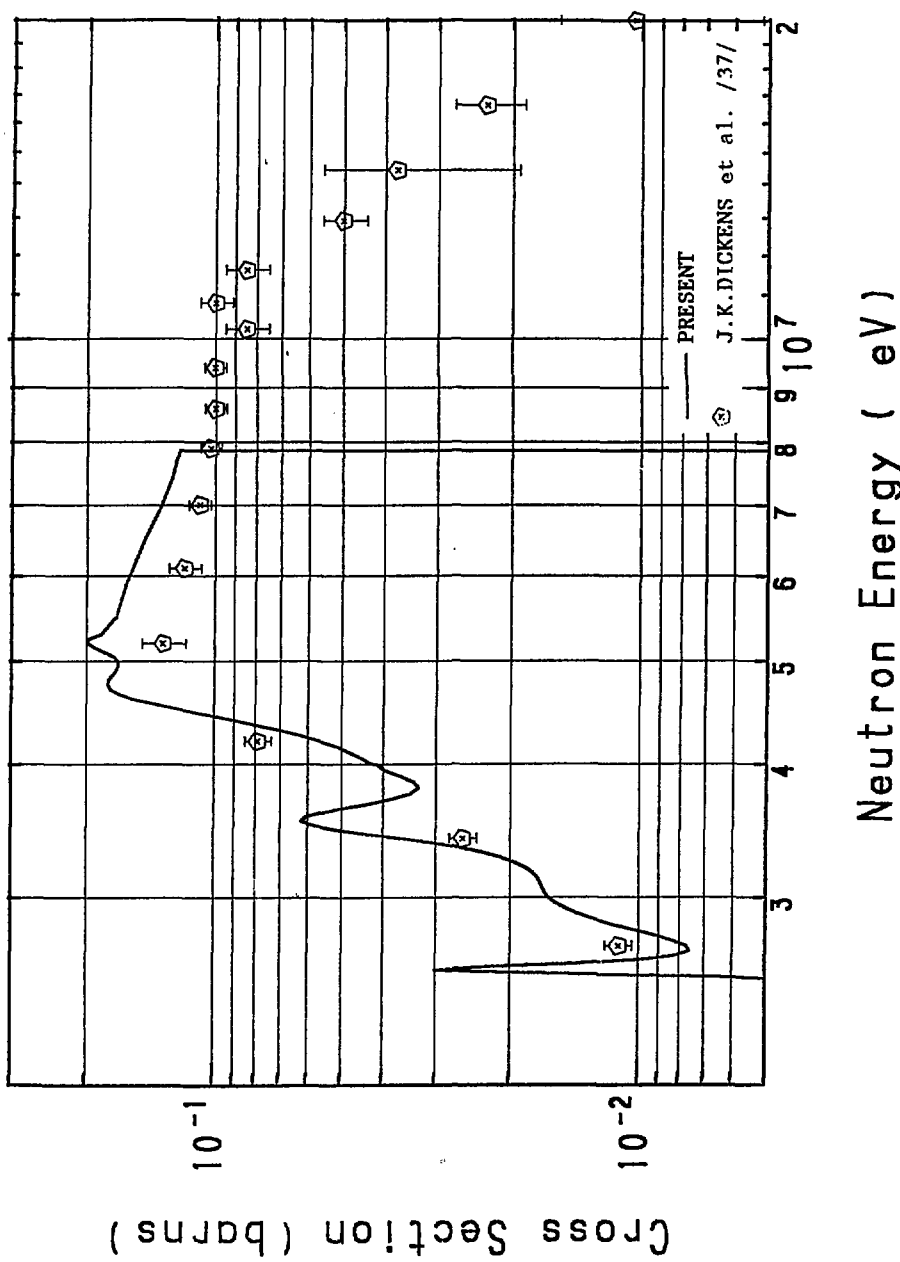


Fig.11 γ -ray Production Cross Section for the γ -ray Energy of 2.125
MeV